 doi:10.20944/preprints202208.0438.v1

Article

A Systematic Approach to Thermochemical Treatment of Municipal Household Solid Waste into Valuable Products: Analysis of Routes, Gravimetric Analysis, Pre-Treatment of Solid Mixtures, Thermochemical Processes, and Characterization of Bio-Oils and Bio-Adsorbents

Fernanda Paula da Costa Assunção[1], Diogo Oliveira Pereira[1], Jéssica Cristina Conte da Silva[1], Jorge Fernando Hungria Ferreira[1], Kelly Christina Alves Bezerra[1], Lucas Pinto Bernar[2], Caio Campos Ferreira[2], Augusto Fernando de Freitas Costa[2], Lia Martins Pereira[2], Simone Patrícia Aranha da Paz[2], Marcelo Costa Santos[2], Raise Brenda Pinheiro Ferreira[3], Beatriz Rocha Coqueiro[3], Aline Christian Pimentel Almeida[3], Neyson Martins Mendonça[3], José Almir Rodrigues Pereira[3], Sílvio Alex Pereira da Mota[4], Douglas Alberto Rocha de Castro[5], Sergio Duvoisin Jr.[6], Antônio Augusto Martins Pereira Jr.[7], Luiz Eduardo Pizarro Borges[7] and Nélio Teixeira Machado[1,2,3]*

[1] Graduate Program of Civil Engineering, Campus Profissional-UFPA, Universidade Federal do Pará, Rua Augusto Corrêa N° 1, Belém 66075-110, Brazil; fernanda.assuncao.itec@gmail.com (F.P.d.C.A.); diogooliveirapereira@gmail.com (D.O.P.); jessica.conte.silva@itec.ufpa.br (J.C.C.d.S); fernandohughes13@hotmail.com (J.F.H.F); kelly.bezerra@itec.ufpa.br (K.C.A.B.)

[2] Graduate Program of Natural Resources Engineering of Amazon, Campus Profissional-UFPA, Universidade Federal do Pará, Rua Augusto Corrêa N° 1, Belém 66075-110, Brazil; lucas.bernar7@gmail.com (L.P.B.); caiocf7@hotmail.com (C.C.F.); affreitas@ufpa.br (A.F.d.F.C.); liapereira@ufpa.br (L.M.P.); paz@ufpa.br (S.P.A.d.P.); marcelo.santos@ufra.edu.br (M.C.S.)

[3] Faculty of Sanitary and Environmental Engineering, Campus Profissional-UFPA, Universidade Federal do Pará, Rua Corrêa N° 1, Belém 66075-900, Brazil; raise.ferreira@itec.ufpa.br (R.B.P.F.); beatriz.coqueiro@itec.ufpa.br (B.R.C.); alinecpas@ufpa.br (A.C.P.A.); neysonmm@ufpa.br (N.M.M.); rpereira@ufpa.br (J.A.R.P.);

[4] Graduate Program of Chemistry, Universidade Federal do Sul e Sudeste do Pará, Folha 31, Quadra 7, Lote Especial - Nova Marabá, CEP: 68.507.590, Marabá/PA, Brasil, silviomota@unifesspa.edu.br (S.A.P.d.M.)

[5] Centro Universitário Luterano de Manaus – CEULM/ULBRA, Avenida Carlos Drummond de Andrade N°. 1460, Manaus 69077-730, Brazil; douglascastro87@hotmail.com (D.A.R.d.C.)

[6] Faculty of Chemical Engineering, Universidade do Estado do Amazonas-UEA, Avenida Darcy Vargas N°. 1200, Manaus 69050-020, Brazil; sjunior@uea.edu.br (S.D.Jr.)

[7] Laboratory of Catalyst Preparation and Catalytic Cracking, Section of Chemical Engineering, Instituto Militar de Engenharia-IME, Praça General Tibúrcio N°. 80, Rio de Janeiro 22290-270, Brazil; antonio.augusto@ime.eb.br (A.A.M.P.J), luiz@ime.eb.br (L.E.P.B.)

* Correspondence: machado@ufpa.br; Tel.: +55-91-984-620-325

Abstract: This work aims to investigate the effect of process temperature and catalyst content by pyrolysis and thermal catalytic cracking of (organic matter + paper) fraction from municipal household solid waste (MHSW) on the yields of reaction products (bio-oil, bio-char, H_2O, and gas), acid value and chemical composition of bio-oils, and characterization of bio-chars, in laboratory scale. The collecting sectors of MHSW in the municipality of Belém-Pará-Brazil were chosen based on geographic and socio-economic database. The MHSW collected and transported to the segregation area. The gravimetric analysis of MHSW carried out and the fractions (*Paper, Cardboard, Tetra Pack, Hard Plastic, Soft Plastic, Metal, Glass, Organic Matter, and Inert*) separated. The selected organic matter and paper submitted to pre-treatment of crushing, drying, and sieving. The experiments carried out at 400, 450, and 475 °C and 1.0 atmosphere, and at 475 °C and 1.0 atmosphere, using 5.0, 10.0, and 15.0% (wt.) $Ca(OH)_2$, in batch mode. The bio-oil characterized for acid value. The chemical functions present in bio-oil identified by FT-IR and the composition by GC-MS. The bio-char characterized by SEM, FT-IR and XRD. The variance in mass

(wt.%) for organic fraction of municipal household solid waste, *between 56.21 and 67.45% (wt.)*, lies with the interval of 56% (wt.) and 64% (wt.) of OFMHSW for middle and low income countries. The pyrolysis of MHSW fraction (organic matter + paper) show bio-oil yields between 2.63 and 9.41% (wt.), aqueous phase yields between 28.58 and 35.08% (wt.), solid phase yields between 35.29 and 45.75% (wt.), and gas yields between 16.54 and 26.72% (wt.). The bio-oil yield increases with pyrolysis temperature. For the catalytic cracking, the bio-oil and gas yields increase slightly with CaO content, while that of bio-char decreases, and the H_2O phase remains constant. The GC-MS of liquid reaction products identified the presence of hydrocarbons (alkanes, alkenes, alkynes, cycloalkanes, and aromatics) and oxygenates (carboxylic acids, ketones, esters, alcohols, phenols, and aldehydes), as well as compounds containing nitrogen, including amides and amines. The acidity of bio-oil decreases with increasing process temperature and with aid $Ca(OH)_2$ as catalyst. The concentration of hydrocarbons in bio-oil increases with increasing $Ca(OH)_2$-to-MHSW fraction ratio due to the catalytic deoxygenation of fatty acids molecules, by means of de-carboxylation/de-carbonylation, producing aliphatic and aromatic hydrocarbons.

Keywords: MHSW; Organic fraction from MHSW, Thermal processing; Bio-char characterization; Bio-oil: Liquid hydrocarbons

1. Introduction

In a global consumer society whereas the production of household solid wastes has been increasing in the last years [1], the disposal of municipal household solid wastes (MHSW) poses a global challenge for medium and large cities as it involves complex logistics, safety, environment and energetic aspects for its adequate management [2], not only for high income countries but particularly for medium and low income countries [3-5].

Among the technologies available for proper treatment & transformation of municipal household solid wastes (MHSW), including biological, physicochemical and thermal treatment [6-7], pyrolysis has a great potential not only for the thermochemical transformation of MHSW fractions such as residual biomass [8], thermoplastic polymers [9], plastics (hard, soft) [10-11], cardboard [12-13], recycled paper [14], non-recycled paper [15], and organic matter [16-17], but also for MSW [18-27], and the literature reports numerous studies on the subject [6-25].

Among the catalysts applied by the pyrolysis of MHSW fractions (residual biomass, thermoplastic polymers, plastics (hard, soft), cardboard, recycled paper, non-recycled paper, organic matter. Etc.) and MSHW, the most used were zeolite [18, 22], Kaolin [21-22], HZSM-5 [10, 26-27], FCC [26-27], Y-zeolite [26-27], β-zeolite [26-27], $Al(OH)_3$ [26-27], Ni-Mo [26-27], MoO_3 [26-27], ZSM-5 [10], NH4ZSM-5 [10], CaO [28-29], ZnO [30], Fe_2O_3 [30], CuO [30], Al_2O_3 [30], calcined calcite (CaO) [31], and calcined dolomite (MgO.CaO) [18, 31].

The state of art, progress, new trends and tendencies on pyrolysis and catalytic cracking of MHSW fractions and MSHW were described in details on the excellent reviews of *Hasan et al.* [25], *Chen et. al.* [32], *Sipra et. al*. [33], and *Lu et. al*. [34].

The studies on pyrolysis and catalytic cracking of MHSW fractions and MSHW were focused on the yields of reaction products [5, 12-13, 17-19], bio-char characterization [5, 15-17, 27, 31], bio-oil properties and composition [11-12, 17, 19, 21-28], composition of gaseous phase [12-13, 18, 20, 23-24, 26, 28, 31], reaction kinetics [10, 12-16, 19, 30-31], as well as reaction mechanism/pathway [17].

 doi:10.20944/preprints202208.0438.v1

The pyrolysis and catalytic cracking of MHSW fractions and MSHW have been carried out by flash pyrolysis [10, 16, 28, 31], as well as by vacuum pyrolysis [19], fixed bed reactors [5, 12-15, 17-19, 21-24, 26-27], and fluidized bed reactors [20].

The pyrolysis and catalytic cracking of MHSW fractions and MSHW were performed in micro [15], laboratory [10, 12-14, 16-24, 26-28, 30-31], and pilot scales [5, 8]. The processes operated in batch [5, 10, 12-19, 21-24, 26-28, 30-31], and continuous mode [20, 23], and only one study operated as a two-stage reactor [31].

The reaction products by pyrolysis and thermal catalytic cracking of MHSW fractions (residual biomass, thermoplastic polymers, plastics (hard, soft), cardboard, recycled paper, non-recycled paper, and organic matter) [8-17], and MSHW [18-27, 28-29, 31], includes a bio-oil, an aqueous acid phase, a gaseous phase, and a solid phase (bio-char) [8-9, 11-13, 16-24, 26-27, 28-29, 31].

The pyrolysis bio-oils from MSW fractions and MSW were physicochemical characterized for density [8-9, 19, 21-22], kinematic viscosity [8-9, 19, 21-22], flash point [19, 21-22], pour point [19, 22], water content [19, 21-22], oil content [19, 21-22], solids content [21-22], ash content [19], sulfur content [19], nitrogen content [19], cetane/octane number [21-22], HHV [19], acid value [8, 19], refractive index [9], and pH [19].

The bio-oil obtained by pyrolysis and catalytic cracking of MHSW fractions and MSHW were composed by alkanes, alkenes, ring-containing alkanes, ring-containing alkenes, cycle-alkanes, cycle-alkenes, aromatics , and oxygenates including phenols, aldehydes, ketones, sugars, amines, amides, ethers, esters and alcohols [8, 11-12, 17, 19, 21-28].

Beyond the operating mode (batch, continuous), type of pyrolysis process (flash and slow pyrolysis, and vacuum pyrolysis), type of reactors (fixed bed reactors and fluidized bed reactors), as well as process schema (two-stage reactor), other process parameters/variables that may affect the yields and quality of bio-oil by pyrolysis and catalytic cracking of MHSW fractions and MSHW are temperature [12-16, 18-19, 23-24, 26-27, 30-31], catalyst-to-MHSW [28] and characteristics of feed material [5, 12-15, 28].

Despite some studies focusing the effect of temperature and catalyst-to-MHSW ratio on the yield and chemical composition of bio-oil produced by pyrolysis and catalytic cracking of MHSW fractions and MSHW performed in micro [15], laboratory [10, 12-14, 16-24, 26-28, 30-31], and pilot scales [5, 8], *until the moment, no systematic study has investigated the effect of temperature and catalyst-to-MHSW/fraction ratio on the bio-char morphology and crystalline structure, as well as on the yield of reaction products, chemical composition and acidity of bio-oils obtained by pyrolysis and catalytic cracking of (organic matter + paper) fraction from MHSW fractions in laboratory scale with $Ca(OH)_2$ as catalyst*.

The objective of this work was to systematically investigate the effect of temperature and catalyst-to-MHSW/fraction ratio (0.05, 0.10, 0.15) by pyrolysis and catalytic cracking of (organic matter + paper) fraction of MHSW at 400, 450, and 475 °C and 1.0 atmosphere, and at 475 °C and 1.0 atmosphere, using 5.0, 10.0, and 15.0% (wt.) $Ca(OH)_2$, in batch mode, laboratory scale, on the yields of reaction products (bio-oil, bio-char, H_2O, and gas), acid value and chemical composition of hydrocarbons (alkanes, alkenes, alkynes, ring containing alkanes, and aromatics) and oxygenates (carboxylic acids, alcohols, amines, amides, aldehydes, esters, ketones, phenols, nitrogenous compounds, chlorinated compounds) present within the bio-oils, as well as on the bio-char morphology and crystalline structure.

2. Materials and Methods

 doi:10.20944/preprints202208.0438.v1

2.1. *Strategy and methodology*

The process flowsheet illustrated in Figure 1 summarizes the applied strategy, as well the process methodology, described as a logical sequence of ideas, methods, and procedures to sustainable disposal and thermal treatment of *Municipal Solid Wastes* (MSW) into activated carbon and bio-oil by pyrolysis and catalytic cracking in laboratory scale. First, based on geographic and socio-economic database (IBGE 2010), the collecting sectors of MSW in the municipality of Belém-Pará-Brazil, has been chosen. Then, the MSW collected and transported to the segregation area. Afterwards, the gravimetric analysis of MSW carried out and the material (*Paper, Cardboard, Tetra Pack, Hard Plastic, Soft Plastic, Metal, Glass, Organic Matter, and Inert*) separated. Then, the selected organic matter submitted to drying. Afterwards, the selected paper crushed together with dried organic matter. Then, the crushed material was sieved and conditioned in a freezer. Before the thermal processing, the feezed material was dried again. The thermal transformation experiments were carried out in laboratory scale. The effect of temperature and catalyst-to-(organic matter + paper) were analyzed. The density, acidity and composition of bio-oil determined. The solid phase (bio-adsorbent) was characterized.

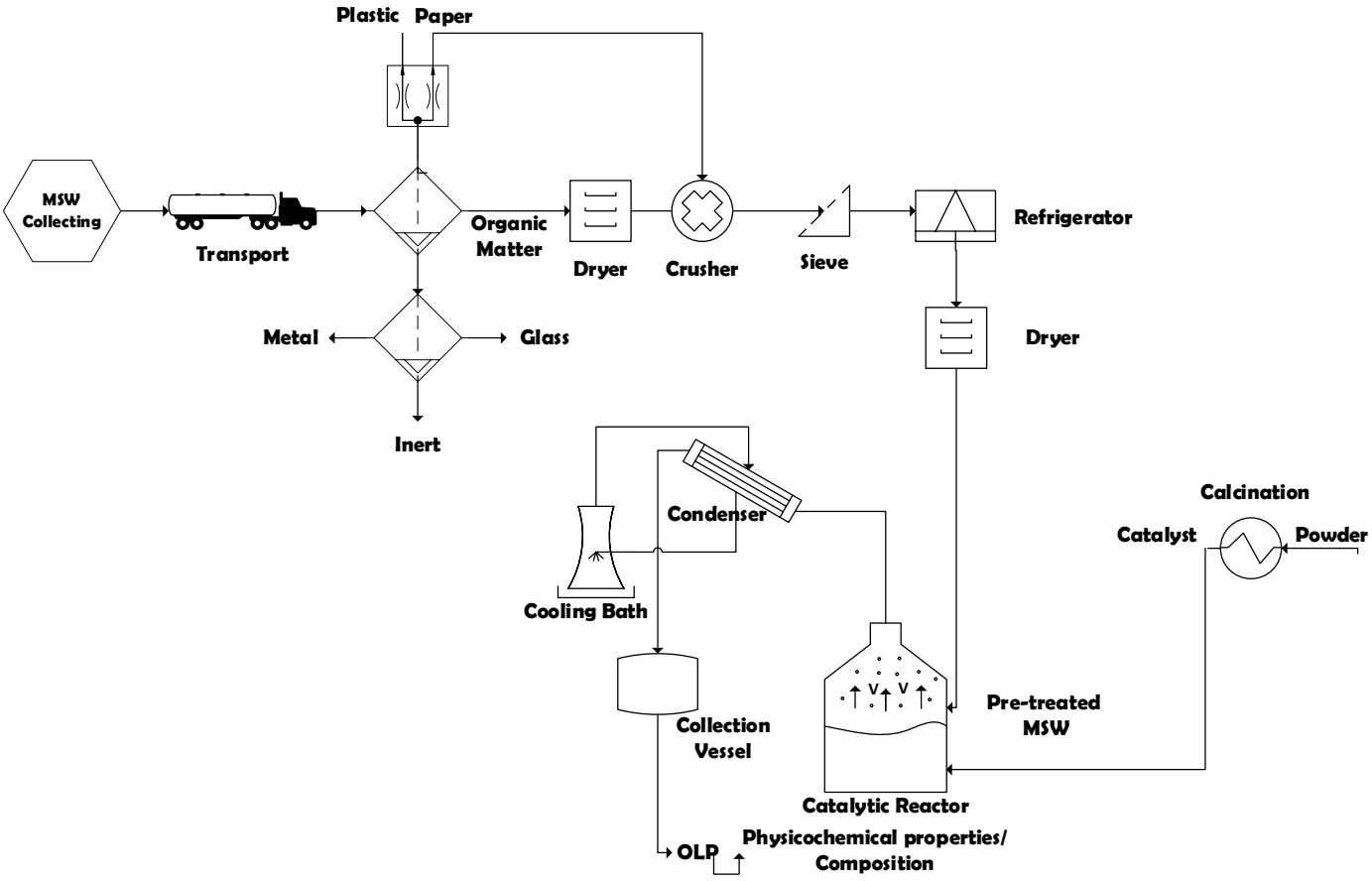

Figure 1. Process flowsheet by collecting, classification/segregation, and pre-treatment of MSW and thermal processing of pre-treated (organic matter + paper) at 400, 450, and 475 °C, 1.0 atm, 0.0, 5.0, 10.0, and 15.0% (wt.) of $Ca(OH)_2$, in laboratory scale.

2.2. *Conceptual design*

The plan of action applied to systematically study the sustainable disposal and thermal treatment of *Municipal Household Solid Wastes* (MHSW) was de-

 doi:10.20944/preprints202208.0438.v1

signed conceptually as a logic sequence of ideas, concepts, and methods including the *choice of a statistically representative route (socio-economic and geographic database)*, *simulation of a statistically representative collected mass of a MHSR route*, *application of a realistic and/or real sampling of MHSW, as the MSW is collected door-to-door*, *transport of MHSW residues to a special segregation place*, *selection/classification of MHSR according to the class of materials* (metal, glass, polymers, *carbohydrates + lipids + proteins + fibers = organic matter*, textiles, *aluminum foil + plastic layers + cardboard + plastic caps + bioplastics = tetra pack*, paper, cardboard, *paper tissue + masks + disposal diapers + pads = sanitary household waste*), *centesimal characterization of organic matter*, *pre-treatment of organic matter/paper* (drying, crushing, sieving, freezing, drying), *thermochemical processing* (pyrolysis, catalytic cracking), characterization of reaction products (bio-oil, bio-adsorbent).

2.2.1 *Selection of routes*

Table 1. Socio-economic classification in the municipality of Belém-Pará-Brazil based on minimum salary [35].

Socio-economic Classification	
Classes	Family Income (Minimum/Basic Salary)
A	over 20 salaries
B	from 10 to 20 salaries
C	from 10 to 20 salaries
D	from 10 to 20 salaries
E	up to 02 salaries

Table 2. Socio-economic classification, population, and average family income in reais (R$) of all the neighborhoods in the municipality of Belém-Pará-Brazil [35].

Neighborhood	**Average Family Income (R$)**	**Population**	**Socio-economic Classes**
Aura	354.51	1.827	E
Águas Lindas	344.47	17.520	E
Curió-Utinga	708.53	16.642	E
Guanabara	381.58	1.588	E
Castanheira	748.87	24.424	E
Souza	1291.02	13.190	D
Marco	1326.37	65.844	D
Canudos	821.81	13.804	E
Terra Firme	414.65	61.439	E
Guamá	525.80	94.610	E
Condor	483.06	42.758	E
Jurunas	633.08	64.478	E
Fátima	656.14	12.385	E
Umarizal	1991.17	30.090	D
São Brás	1971.37	19.936	D
Cremação	1093.94	31.264	D
Batista Campos	2537.63	19.136	C
Nazaré	3036.30	20.504	C
Reduto	2964.30	6.373	C
Campina	2035.60	6.156	D
Cidade Velha	1235.27	12.128	D
Total	-	**576.096**	-

The strategy applied for the selection of collecting routes in the municipality of Belém-Pará-Brazil is described synthetically as follows. The company Terraplena Ltda (Belém-Pará-Brazil) collects urban solid waste in the Metropolitan

Preprints (www.preprints.org) | NOT PEER-REVIEWED | Posted: 26 August 2022 doi:10.20944/preprints202208.0438.v1

Region of Belém-Pará-Brazil, containing a total of 37 routes. In order to reduce the size of the sample collection space, route 1202 was chosen, corresponding to the neighborhoods of *Cremação* and *Guamá*. These neighborhoods have socio-economic and demographic characteristics stratified into Class D and E, respectively, according to IBGE in 2010 [35], shown in Table 1. Furthermore, *adding the average per capita family income of the Classes D and E of all the neighborhoods of Belém gives 85.71%*. In addition, *by adding the population of all the neighborhoods in the municipality of Belém that include classes D and E, gives a population percentage of 92.01%*, as shown in Table 2. In this sense, based on the facts described above, *route 1202* was chosen in order to significantly represent the gravimetric analysis of urban solid waste in the municipality of Belém-Pará-Brazil.

The Cremação neighborhood is located in the developed urban center and borders the neighborhoods of Nazaré, São Brás and Batista Campos. It has a population of 31264 inhabitants with a per capita income of R$1093.90, according to IBGE in 2010 [35], therefore, it belongs to the socio-economic Class D. Its area includes fairs, shops, schools, residential buildings and houses. The Guamá neighborhood is the most populous in the municipality of Belém-Pará-Brazil, with 94610 inhabitants, as well as an average per capita income of R$525.80, belonging to the socio-economic Class E. Its area is much diversified, containing a commercial sector, a fair, as well as schools and residential houses.

The collecting points (green circles) of municipal household solid wastes (MHSW) are described in Figure 2 and the spatial coordinates (Longitude-X, Latitude-Y) of each point described in Table 3. The collection points, 27 (twenty-seven) in total, were randomly selected in order to diversify the sampling of MHSW in each neighborhood, based on the methodology described in the literature by Nunes (2015) [36].

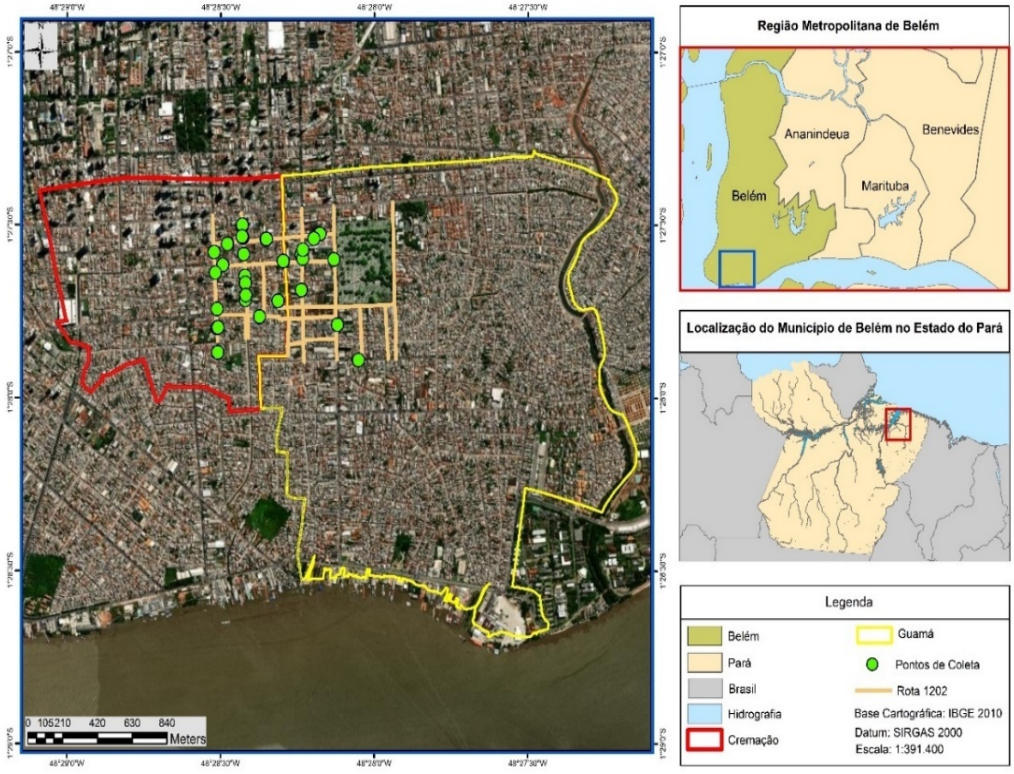

Figure 2. Collecting points (green circles) of municipal household solid waste (MHSW) in the neighborhoods of *Cremação* and *Guamá* in the city of Belém-Pará-Brazil on 18/10/2021, 20/10/2021, 27/10/2021, and 29/10/2021.

 doi:10.20944/preprints202208.0438.v1

Table 3. Coordinates (Longitude-X, Latitude-Y) of each collecting points (green circles) (Longitude-X, Latitude-Y) of municipal household solid waste (MHSW) in the neighborhoods of *Cremação* and *Guamá* in the city of Belém-Pará-Brazil on 18/10/2021, 20/10/2021, 27/10/2021, and 29/10/2021.

Day	Collecting points	Coordinates (UTM)	
		X	Y
18/10/2021	1	780950.42	9837973.32
	2	781119.90	9838278.16
	3	781009.64	9838551.67
	4	781568.34	9838605.03
	5	781463.30	9838472.94
20/10/2021	6	781103.21	9838585.31
	7	781117.53	9838342.88
	8	780928.98	9838507.28
	9	781010.98	9838551.89
	10	781242.17	9838575.64
	11	781244.84	9838577.52
	12	781098.10	9838591.18
27/10/2021	13	780980.57	9838439.40
	14	780946.68	9838204.78
	15	781116.87	9838252.38
	16	781099.50	9838652.80
29/10/2021	17	781455.46	9838305.47
	18	781800.80	9837931.59
	19	781453.34	9838493.90
	20	781560.25	9838606.52
	21	781652.42	9838468.44
	22	781673.83	9838119.49
	23	780947.53	9838102.46
	24	781115.51	9838380.92
	26	781107.30	9838497.16
	27	781096.49	9838642.49

2.2.2 *Simulation of sample mass of MHSR*

In order to compute the statistically representative sample volume of MHSW, a simulation was performed with aid the software StatDisk 13.0. The simulation was based on the volume collected by route using a collector truck of 15 m^3, assuming that average density of MHSW was that of liquid water. The significance and confidence levels were set equal to 5% and 95%, respectively, with a margin of error of 10%, *giving as result a sample of mass ≈100 kg [37].*

2.2.3 *Sampling, transport and segregation of MHSW*

In order preserve the original characteristics of MHSW, that is, the MHSW before mixing and compaction, which not only causes loss mass by dewatering but also a rapid degradation of organic matter, as well as production of leachate with huge loads of contaminants, the collecting of MHSW samples were carried out door-to-door. The collections of MHSW on route 1202 were carried out on the 18th, 20th, 27th, and 29/10/2021. The samples were packed in plastic bags with

 doi:10.20944/preprints202208.0438.v1

a capacity of 200 kg and transported using an appropriate vehicle to prevent the material from being compacted. Afterwards, the plastic bags of MHSW placed over a waterproofed surface inside the UFPA's Sludge and Composting Experimental Laboratory, as shown in Figure 3. Finally, the HHSW were *selected/classified manually* and weighed using a digital balance (Welmy, São Paulo-Brazil, Model: W200/50).

Figure 3. Municipal household solid wastes over a waterproofed surface inside the UFPA's Sludge and Composting Experimental Laboratory.

2.3. Materials

2.3.1. Mixture of organic matter and papers

The organic matter, a mixture of *carbohydrates, lipids, proteins, and fibers*, selected from municipal household solid waste (MHSW), was submitted to pre-treatment (drying, crushing, sieving) and conditionate in a freezer to avoid physicochemical and microbiologic degradation. Figure 4 shows the organic matter before drying, organic matter after drying and papers before crushing.

Figure 4. Organic matter and paper used as feed material by thermal processing in laboratory scale. Organic matter before drying (a), organic matter after drying (b), and papers before crushing (c).

The selected/segregated paper from MHSW were crushed together with dried organic matter. Afterwards, the mixture of organic matter and paper was sieved and conditioned in a freezer. The pre-treated mixture of organic matter and paper used as feed material by thermal processing is shown in Figure 5.

Figure 5. Pre-treated organic matter + paper used as feed material by thermal processing in laboratory scale. Organic matter + paper after crushing (a), organic matter + paper after sieving (b).

 doi:10.20944/preprints202208.0438.v1

2.3.2. Pre-treatment of organic matter and papers

The selected/classified organic matter was submitted to drying at 105 °C for 24 hours using an analogic controlled oven (DeLeo, Brasil, Model:). Then, the dried organic matter was crushed together with paper using a grain/straw knife mill (TRAPP, Brazil, Model: TRF 600). Afterwards, the milled/crushed mixture of organic matter and paper was sieved using a series of sieves (4.0, 6.0, 12, and 14 mesh). A total of 04 (four) batches of pre-treated organic matter + paper, one for each MHSW collecting, was carried out.

2.3.3. Centesimal and physicochemical characterization of organic matter and papers

The dried, crushed and sieved organic matter was subjected to centesimal characterization for lipids, proteins, moisture, and ash according to official methods AOCS 963.15, AOCS 991.20, AOCS 935.29 and ASTM D 3174-04 [8, 38]. In addition, pH and electrical conductivity has been also measured according to ASTM D1293-18 and ASTM D 1125-14 [39].

2.4. Experimental apparatus and procedures

2.4.1. Experimental apparatus

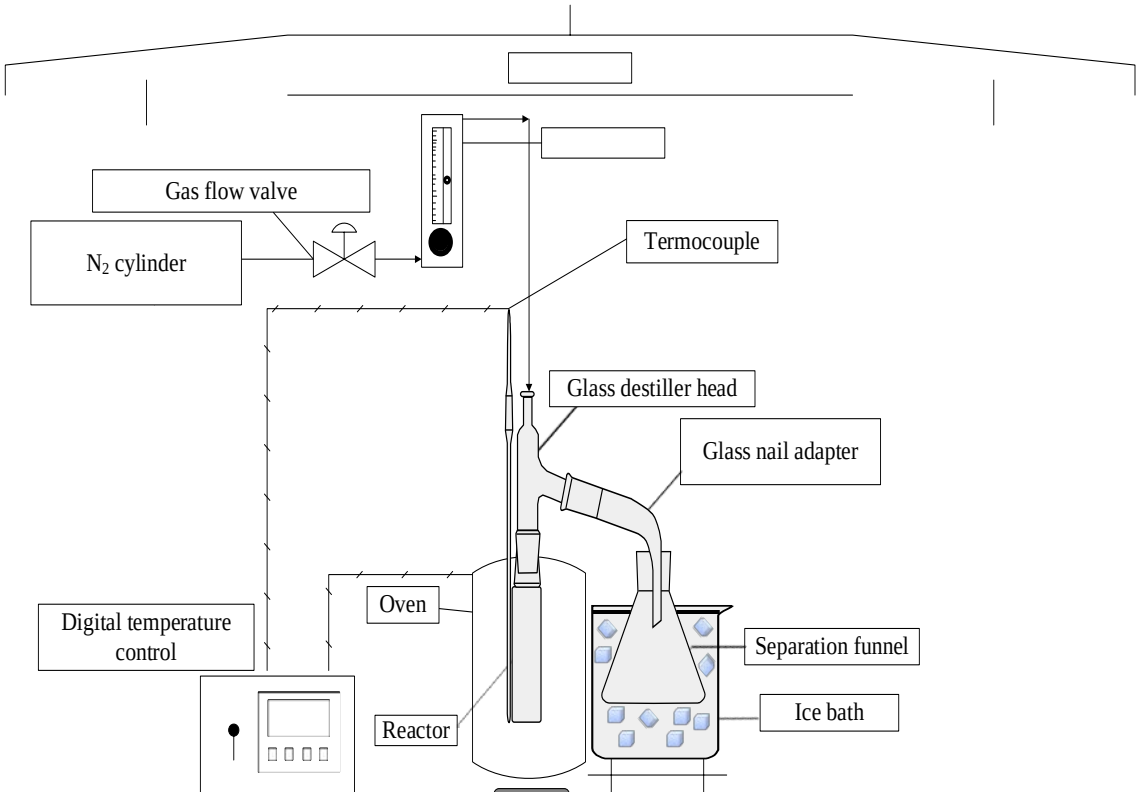

Figure 6. Schema of laboratory scale borosilicate glass reactor.

The schematic diagram of borosilicate glass reactor in laboratory scale is shown in Figure 6. The experimental apparatus contains a cylindrical reactor of 200 mL, a Liebig glass condenser, a ceramic heating system of 800 W, and a digital temperature control (Therma, Model: TH90DP202-000), as described in details elsewhere [8, 40-41].

2.4.2. Experimental procedures

By the pyrolysis of pre-treated solid mixture of organic matter + paper, approximately 50.0 g weighed using a semi-analytical balance (Marte, São-Paulo-Brazil, Model: AL500). After sealing the reactor, the experimental apparatus has been set up. Then, the cooling system is turned on and the water temperature

 doi:10.20944/preprints202208.0438.v1

was set at 10 °C. Afterwards, the desired heating rate (10 °C/min), and temperature (400, 450, and 475 °C) were set-up. The reactor temperature was recorded every 10 minutes. The mass of liquid phase and coke were collected and weighed, and the mass of gas computed by difference. The bio-oil was separated from aqueous phase by decantation inside the separation funnel. Afterwards, the bio-oil physicochemical characterized by density and acidity.

By the thermal catalytic cracking experiments, calcium hydroxide ($Ca(OH)_2$) was mixed with pre-treated organic matter + paper using a glass Becker of 250 mL. The thermal catalytic cracking experiments carried out with 5.0, 10.0, and 15.0% (wt.) $Ca(OH)_2$. Afterwards, the mixture place inside the reactor, as depicted in Figure 7. Then, the desired heating rate (10 °C/min), and temperature (475 °C) were set-up. The reactor temperature was recorded every 10 minutes. The mass of liquid phase and coke were collected and weighed, and the mass of gas computed by difference. The bio-oil was separated from aqueous phase by decantation inside the separation funnel. Afterwards, the bio-oil physicochemical characterized by density and acidity.

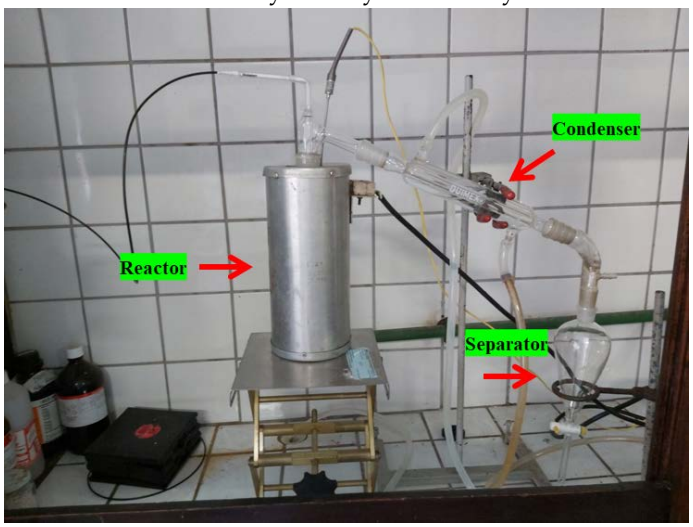

Figure 7. Experimental apparatus (glass reactor in laboratory scale).

2.6. Physicochemical and chemical composition of bio-oil

2.6.1. Physicochemical characterization of bio-oil and aqueous phase

The bio-oil was characterized for acidity according to AOCS Cd 3d-63. In addition, the aqueous phase was characterized for acidity by AOCS Cd 3d-63 and density by the pycnometer method ASTM D854 at 25 °C, as described elsewhere [8, 40-43].

2.6.2. Chemical composition of bio-oil and aqueous phase

The chemical composition of bio-oil and aqueous phase were determined by GC-MS and the equipment and procedure described in details by Castro *et. al.* [8, 44-45]. The concentrations were expressed in area, as no internal standard was injected for comparison the peak areas. In addition, the qualitative analysis of chemical functions present in bio-oil were performed by FT-IR [8, 40-42].

2.7. Characterization of bio-char

2.7.1. SEM and EDS analysis

The morphological characterization of bio-char obtained by thermal catalytic cracking with 5.0, 10.0, and 15.0% (wt.) $Ca(OH)_2$) of organic matter + paper were performed by scanning electron microscopy using a microscope (Tescan GmbH, Czech Republic, Model: Vega 3). The samples were covered with a thin layer of gold using a Sputter Coater (Leica Biosystems, Germany, Model: Balzers

 doi:10.20944/preprints202208.0438.v1

SCD 050). Elemental analysis and mapping were carried out by energy dispersive x-ray spectroscopy (Oxford instruments, UK, Model: Aztec 4.3) [44-45].

2.7.2. XRD analysis

The crystalline characterization of bio-char obtained by thermal processing (pyrolysis and thermal catalytic cracking with 5.0, 10.0, and 15.0% (wt.) $Ca(OH)_2$) of organic matter + paper performed by x-ray diffraction using a diffractometer (Rigaku, Japan, Model: MiniFlex600) at the Laboratory of Structural Characterization (FEMAT/UNIFESSPA) and the equipment specifications described as follows: *generator* (maximum power: 600 W; tube voltage: 40 kV; tube current: 15 mA; X-ray tube: Cu), *optics* (fixed divergence, scattering and receiving slit; filter; Kβ sheet; monochromator: graphite; soller slit: 5.0°), *goniometer* (model: vertical, radius: 150 mm, scanning range: -3 A , 145° (2θ); scanning speed: 0.01 to 100°/min (2θ); accuracy: ± 0.02°) and *detector* (high-speed silicone tape) [44-45].

2.8. Mass balances by catalytic of organic matter and paper

Application of mass conservation principle in the form an overall mass balance within the pyrolysis/catalytic reactor, operating in batch mode, open thermodynamic system, yields the following equations [45].

$$\dot{m}_{in,pyrolysis/catalytic} - \dot{m}_{out,pyrolysis/catalytic} = \frac{dm_{Feed}}{d\tau} \quad (1)$$

$$\dot{m}_{in,pyrolysis/catalytic} = 0 \quad (2)$$

$$-\dot{m}_{out,pyrolysis/catalytic} = \frac{dm_{Feed}}{d\tau} \quad (3)$$

$$-\dot{m}_{out,pyrolysis/catalytic} = \dot{m}_{vapors,pyrolysis/catalytic} \quad (4)$$

Where $\dot{m}_{in,pyrolysis/catalytic}$ is the mass flow rate entering the glass reactor, $\dot{m}_{out,pyrolysis/catalytic}$ is the mass flow rate leaving the glass reactor, $\frac{dm_{Feed}}{d\tau}$ is the time rate variation of feed mass inside the glass reactor , $\dot{m}_{vapors,pyrolysis/catalytic}$ is the mass flow rate of pyrolysis/catalytic cracking vapors leaving the glass reactor and entering the condenser. By applying an overall steady state mass balance within the condenser, yields equation (5).

$$\dot{m}_{vapors,pyrolysis/catalyst} = \dot{m}_{gas} + \dot{m}_{bio-oil} \quad (5)$$

Where $\dot{m}_{gas}$ is the mass flow rate of non-condensable gases leaving the condenser, computed by difference, and $\dot{m}_{bio-oil}$ is the mass flow rate of bio-oil collected inside the separation funnel. The mass of solid remaining in the reactor is $\dot{m}_{solid}$. By performing a steady state global mass balance within the control volume consisting of glass reactors, condenser, and separation funnel yields equation (6).

$$\dot{m}_{Feed} = \dot{m}_{solid} + \dot{m}_{gas} + \dot{m}_{bio-oil} \quad (6)$$

The process performance evaluated by computing the yields of bio-oil, solid (coke), and gas defined by equations (7) and (8), and the yield of gas by difference, using equation (9).

$$Y_{bio-oil}[\%] = \frac{M_{bio-oil}}{M_{Feed}} x100 \quad (7)$$

$$Y_{solids}[\%] = \frac{M_{solids}}{M_{Feed}} x100 \quad (8)$$

$$Y_{gas}[\%] = 100 - (Y_{bio-oil} + Y_{solids}) \quad (9)$$

3. Results

3.1. Centesimal characterization of (organic matter + paper) fraction of MHSW

The dried, crushed and sieved fraction of MHSW (organic matter + paper) was subjected to centesimal characterization for lipids, proteins, moisture, ash, pH and electrical conductivity according to official methods AOCS 963.15, AOCS 991.20, AOCS 935.29, ASTM D 3174-04, ASTM D1293-18 and ASTM D 1125-14 [8, 38], and the results depicted in Table 4, compared with similar data reported in the literature [15, 46]. The results show that ash and moisture content

 doi:10.20944/preprints202208.0438.v1

are close to similar data for proximate analysis of MHSW reported in the literature [15, 46].

Table 4. Centesimal characterization for lipids, proteins, moisture, ash, pH and electrical conductivity of dried, crushed and sieved fraction of MHSW (organic matter + paper).

Centesimal characterization	**(wt.%)**	[15]	[46]
Lipids	10.41	-	-
Proteins	11.33	-	-
Moisture	28.74	22.48	-
Ash	6.73	7.36	9.91
Volatile matter	-	-	-
Fixed carbon	-	-	-
Physicochemical characterization			
pH, 27.0 °C (-)	5.77	-	-
Conductivity, 27.2 °C (µS/m)	15.31	-	-

3.2. Characterization of bio-char

3.2.1 SEM analysis

The microscopies, without the pre-treatment of metallization, of bio-char obtained by catalytic cracking of (organic matter + paper) at 475 °C, 1.0 atmosphere, with 5.0% (wt.) $Ca(OH)_2$ depicted in Figure 8 (a) show a carbonized surface (black colored) and granules (white colored) of different sizes scatter over the surface. The carbonized surface (black colored) is due to the thermochemical transformation of (organic matter + paper) fraction of MHSW, while the white colored surface is due to the $Ca(OH)_2$ used as catalysts. The granules (white colored) of different sizes scatter over the surface being are similar to SEM images of $CaCO_3$ (calcite) reported by *Cabrera-Penna et. al.* [47], as well as the SEM images of $Ca(OH)_2$ reported by *Hassani et. al.* [48], and SEM images of bio-char obtained by pyrolysis of MSW reported by *Gopu et. al.* [49]. By increasing the $Ca(OH)_2$ content to 10 and 15% (wt.), one observes that the granules (white colored) of different sizes spreads over the surface, covering the carbonized surface, as shown in Figures 9 (a) and 10 (a). The higher the $Ca(OH)_2$ content by catalytic cracking of (organic matter + paper) at 475 °C, 1.0 atmosphere, the higher the surface of carbonized surface (black colored) covered by the granules (white colored).

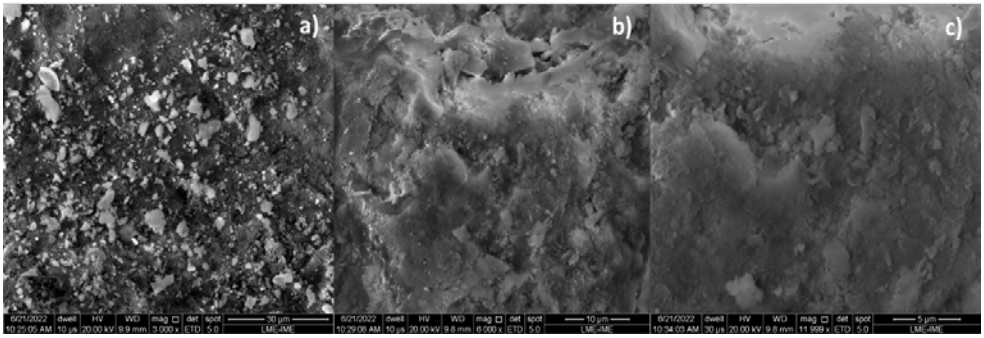

Figure 8. SEM of bio-char obtained by thermal catalytic cracking of (organic matter + paper) fraction of MHSW at 475 °C, 1.0 atmosphere, with 5.0% (wt.) $Ca(OH)_2$ [MAG: 5999 x (a); MAG: 3000 x (b); MAG: 11999 x (c)].

Preprints (www.preprints.org) | NOT PEER-REVIEWED | Posted: 26 August 2022 doi:10.20944/preprints202208.0438.v1

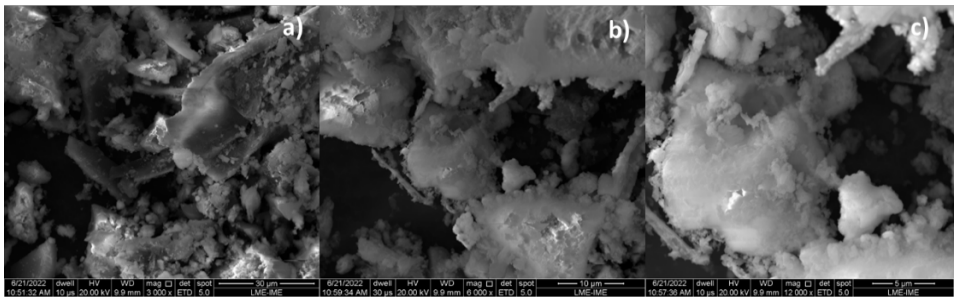

Figure 9. SEM of bio-char obtained by thermal catalytic cracking of (organic matter + paper) fraction of MHSW at 475 °C, 1.0 atmosphere, with 10.0% (wt.) $Ca(OH)_2$ [MAG: 3000 x (a); MAG: 6000 x (b); MAG: 12000 x (c)].

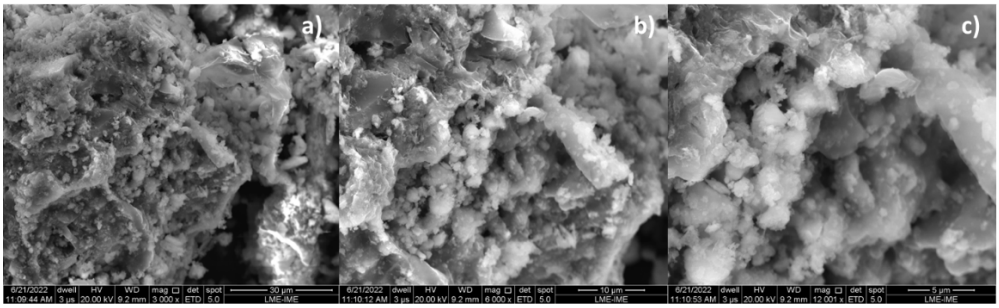

Figure 10. SEM of bio-char obtained by thermal catalytic cracking of (organic matter + paper) fraction of MHSW at 475 °C, 1.0 atmosphere, with 15.0% (wt.) $Ca(OH)_2$ [MAG: 3000 x (a); MAG: 6000 x (b); MAG: 12000 x (c)].

The microscopies, with the pre-treatment of metallization, of bio-char obtained by pyrolysis of (organic matter + paper) fraction of MHSW at 450 °C, 1.0 atmosphere, and by catalytic cracking of (organic matter + paper) fraction of MHSW at 475 °C, 1.0 atmosphere, with 10.0% (wt.) $Ca(OH)_2$, in laboratory scale, illustrated in Figure 11. The SEM images of bio-char by pyrolysis of (organic matter + paper) fraction of MHSW at 450 °C, 1.0 atmosphere, illustrated in Figure 11 (a) shows the formation of porous structure similar to a Bee hive, proving that pyrolysis has changed drastically the morphological structure of (organic matter + paper) fraction of MHSW. In addition, it has not been seen the appearance of granules. On the other hand, the SEM images of bio-char by catalytic cracking of (organic matter + paper) fraction of MHSW at 475 °C, 1.0 atmosphere, with 10.0% (wt.) $Ca(OH)_2$, shows the formation of cavities over the carbonized structure of bio-char, as well as the appearance of granules (white) on the carbonized structure of bio-char. This is due probably to the $Ca(OH)_2$ used as catalysts. The granules (white colored) of different sizes scatter over the surface being are similar to SEM images of $CaCO_3$ (calcite) reported by *Cabrera-Penna et. al.* [47], as well as the SEM images of $Ca(OH)_2$ reported by *Hassani et. al.* [48], and SEM images of bio-char obtained by pyrolysis of MSW reported by *Gopu et. al.* [49].

Preprints (www.preprints.org) | NOT PEER-REVIEWED | Posted: 26 August 2022 doi:10.20944/preprints202208.0438.v1

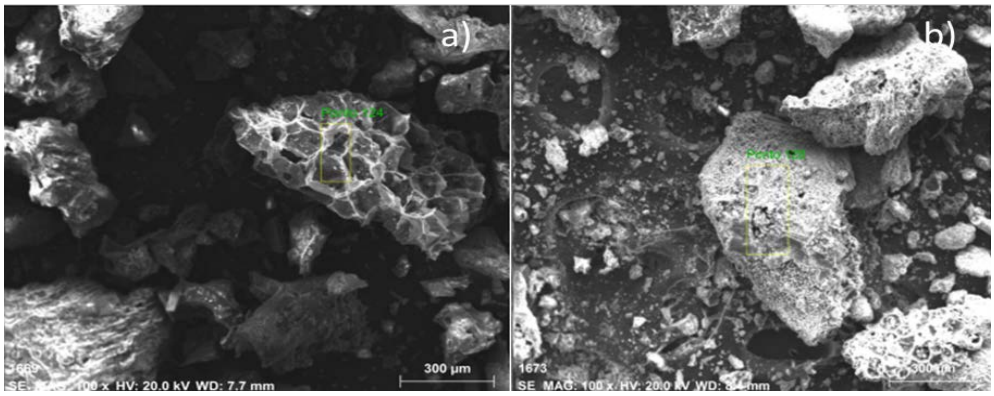

Figure 11. SEM of bio-chars obtained by pyrolysis of (organic matter + paper) fraction of MHSW at 450 °C, 1.0 atmosphere (a), and catalytic cracking of (organic matter + paper) fraction of MHSW at 475 °C, 1.0 atmosphere, with 10.0% (wt.) $Ca(OH)_2$ (b) [MAG: 100 x (a); MAG: 100 x (b)].

3.2.2. EDX analysis

Table 5. Percentages in mass and atomic mass of bio-chars obtained by pyrolysis of (organic matter + paper) fraction of MHSW at 450 °C, 1.0 atmosphere and by catalytic cracking of (organic matter + paper) fraction of MHSW at 475 °C, 1.0 atmosphere, with 10.0% (wt.) $Ca(OH)_2$ as catalyst, in laboratory scale.

	Catalyst					
	Bio-char, Pyrolysis at 450 °C			**Bio-char, Catalytic cracking with 10% (wt.) Ca(OH)2**		
Chemical Elements	Mass [wt.%]	Atomic Mass [wt.%]	SD	Mass [wt.%]	Atomic Mass [wt.%]	SD
C	58.32	77.36	3.00	42.76	60.07	3.83
Ca	12.16	4.84	0.18	21.95	9.24	0.50
Cl	10.24	4.60	0.17	6.07	2.89	0.18
K	8.87	3.62	0.14	3.12	1.35	0.10
O	8.61	8.57	0.62	23.08	24.35	2.30
Na	0.71	0.50	0.05	2.42	1.77	0.14
Fe	0.41	0.12	0.04	--	---	---
Mg	0.33	0.22	0.03	0.01	0.00	0.03
S	0.19	0.10	0.03	0.08	0.04	0.03
Si	0.09	0.05	0.03	0.01	0.01	0.03
Al	0.06	0.03	0.03	0.10	0.06	0.03
P	---	---	---	0.40	0.22	0.04

SD= Standard Deviation

The results of elemental analysis performed by energy dispersive x-ray spectroscopy at a point for bio-chars obtained by pyrolysis of (organic matter + paper) fraction of MHSW at 450 °C, 1.0 atmosphere and by catalytic cracking of (organic matter + paper) fraction of MHSW at 475 °C, 1.0 atmosphere, with 10.0% (wt.) $Ca(OH)_2$ as catalyst, in laboratory scale, are shown in Table 5. The content of carbon in bio-char obtained by catalytic cracking of (organic matter + paper) fraction of MHSW at 475 °C, 1.0 atmosphere, with 10.0% (wt.) $Ca(OH)_2$ as catalyst decreases, while those of oxygen and calcium increase. This is due probably to the reaction of metal oxides present in the (organic matter + paper) fraction of MHSW by thermochemical decomposition at 475 °C, 1.0 atmosphere, with $Ca(OH)_2$, forming $CaCO_3$ (calcite) as proposed by Kumagai *et. al.* [50], for the

Preprints (www.preprints.org) | NOT PEER-REVIEWED | Posted: 26 August 2022 doi:10.20944/preprints202208.0438.v1

thermal degradation of PET, a fraction of MSW, in the presence of $Ca(OH)_2$. The $CaCO_3$ (calcite) in form of granules of different sizes are scattered over the carbonized surface of bio-char during the catalytic cracking of (organic matter + paper) fraction of MHSW at 475 °C, 1.0 atmosphere, decreasing the specific reaction area, and thus making the carbonization of (organic matter + paper) fraction of MHSW difficult. A decrease on the carbon content in the solid phase (carbonaceous residue) by pyrolysis of PET in the presence of $Ca(OH)_2$, was also observed/reported by *Kumagai et. al.* [50]. The oxygen content increases due to the formation of $CaCO_3$ (calcite) by decarboxylation of pyrolysis vapor by CaO, an intermediate reaction product obtained by hydrolysis of $Ca(OH)_2$ [50]. Finally, the calcium content is increased by addition of 10.0% (wt.) $Ca(OH)_2$ as catalyst.

3.2.3. XRD analysis

The XRD analysis of bio-char obtained by pyrolysis of (organic matter + paper) fraction of MHSW at 400 °C, 1.0 atmosphere is shown in Figure 12. The XRD shows the presence of three peaks associated to the crystalline phase $CaCO_3$ (Calcite), one of high intensity on the position 2θ: 29.5 (100%), other of medium intensity on the position 2θ: 20.8 (50%), and a third of low intensity on the position 2θ: 36.6 (16.2%). This is according to the position 2θ: 29.4 (100%), characteristic of $CaCO_3$ rhombohedral phase (PDF 83-1762) [59]. According to *Ghavanati et. al.* [59], the organic fraction of municipal household solid waste contains 4.6 ± 0.6% (wt.) calcium (Ca) on its centesimal composition. Calcium reacts with oxygen to form calcium oxide ($2Ca + O_2 \rightarrow 2CaO$). During the pyrolysis reaction of organic fraction of municipal household solid waste (OFMHSW), carbon dioxide (CO_2) is the major gaseous reaction product formed [26]. Calcite ($CaCO_3$) is formed by carbonation of calcium oxide (CaO) with CO_2 at high temperatures [60]. According to *Kumagai et. al.* [50], calcite ($CaCO_3$) is formed by decarboxylation of OFMHSW pyrolysis vapor compounds containing carboxyl groups, such as carboxylic acids, by CaO [50]. Two peaks were associated to the crystalline phase graphite, a peak of high intensity observed on the position 2θ: 26.7 (100%), while a peak of low intensity identified on the position 2θ: 42.5 (6.7%).

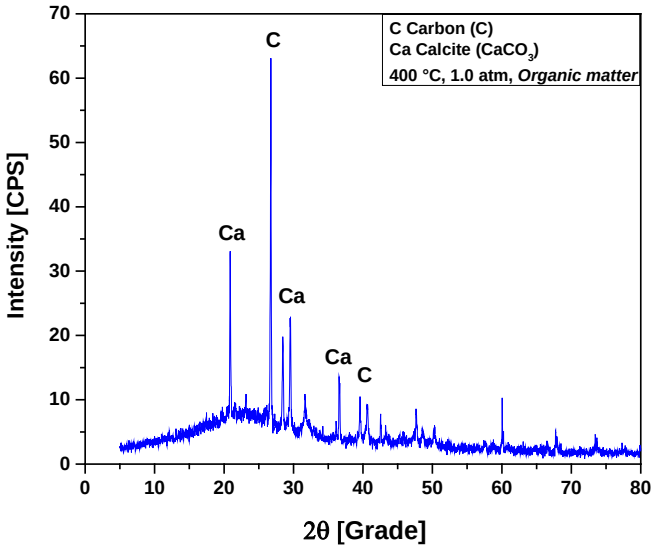

Figure 12. XRD of solid phase products by pyrolysis of (organic matter + paper) fraction of MHSW at 400 °C, 1.0 atmosphere, using a borosilicate glass reactor of 125 mL, in laboratory scale.

Preprints (www.preprints.org) | NOT PEER-REVIEWED | Posted: 26 August 2022 doi:10.20944/preprints202208.0438.v1

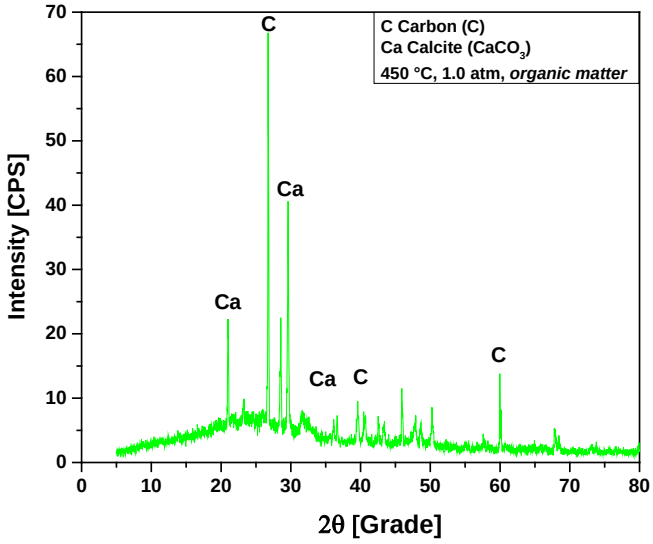

Figure 13. XRD of solid phase products by pyrolysis of (organic matter + paper) fraction of MHSW at 450 °C, 1.0 atm, using a borosilicate glass reactor of 125 mL, in laboratory scale.

The XRD analysis of bio-char obtained by pyrolysis of (organic matter + paper) fraction of MHSW at 450 °C, 1.0 atmosphere, shown in Figure 13, identified the presence of two crystalline phase, $CaCO_3$ (Calcite) and graphite (C). The XRD shows the presence of three peaks associated to the crystalline phase $CaCO_3$ (Calcite), one of high intensity on the position 2θ: 29.5 (100%), other of medium intensity on the position 2θ: 20.8 (50.7%), and a third of low intensity on the position 2θ: 36.6 (16%). Three peaks were associated to the crystalline phase graphite (C), one peak of high intensity observed on the position 2θ: 26.7 (100%) and two peaks of low intensity identified on the positions 2θ: 42.5 (6.7%) and 2θ: 60.0 (15%).

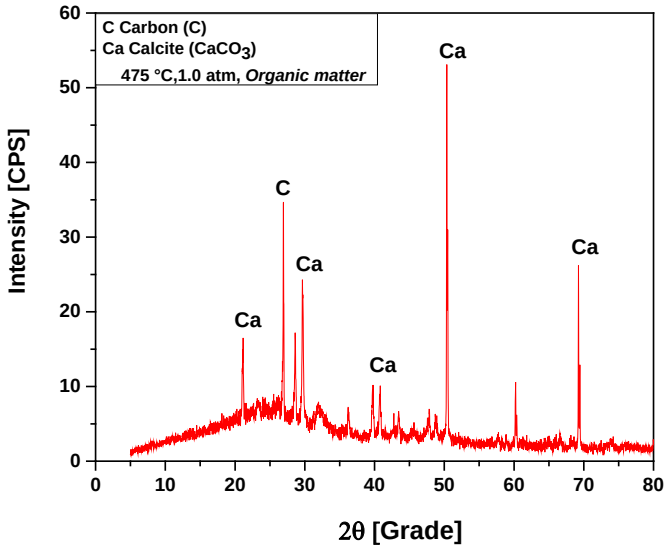

Figure 14. XRD of solid phase products by pyrolysis of (organic matter + paper) fraction of MHSW at 475 °C, 1.0 atm, using a borosilicate glass reactor of 125 mL, in laboratory scale.

Preprints (www.preprints.org) | NOT PEER-REVIEWED | Posted: 26 August 2022 doi:10.20944/preprints202208.0438.v1

The XRD analysis of bio-char obtained by pyrolysis of (organic matter + paper) fraction of MHSW at 475 °C, 1.0 atmosphere, shown in Figure 14, identified the presence of two crystalline phase, $CaCO_3$ (Calcite) and graphite (C). The XRD shows the presence of four peaks associated to the crystalline phase $CaCO_3$ (Calcite), one of high intensity on the position 2θ: 50.3 (100%), one of medium intensity on the position 2θ: 69.2 (48.9%), and two of low intensity on the positions 2θ: 21.1 (22.2%) and 2θ: 29.6 (38.1%). One peak of high intensity is associated to the crystalline phase graphite, observed on the position 2θ: 26.6 (100%).

The XRD analysis of bio-char obtained by catalytic cracking of (organic matter + paper) fraction of MHSW at 475 °C, 1.0 atmosphere, with 5% (wt.) $Ca(OH)_2$, shown in Figure 15, identified the presence of two crystalline phase, $CaCO_3$ (Calcite) and graphite (C). Three peaks are associated to the crystalline phase $CaCO_3$ (Calcite), one of high intensity on the position 2θ: 29.7 (100%), and two of low intensity on the positions 2θ: 20.8 (50.7%), and a third of low intensity on the position 2θ: 39.8 (13.3%) and 2θ: 42.7 (19.4%). Two peaks were associated to the crystalline phase graphite (C), one peak of high intensity observed on the position 2θ: 26.9 (100%) and other of low intensity on the positions 2θ: 50.4 (19.5%). One observes an increase on the peak intensity of $CaCO_3$ (Calcite) due to the use of $Ca(OH)_2$ as catalyst. In fact, $Ca(OH)_2$ reacts at high temperatures losing a H_2O molecule ($Ca(OH)_2 \rightarrow CaO + H_2O$) [50], and $CaCO_3$ is formed by decarboxylation of OFMHSW pyrolysis vapor compounds containing carboxyl groups, such as carboxylic acids, by CaO [50].

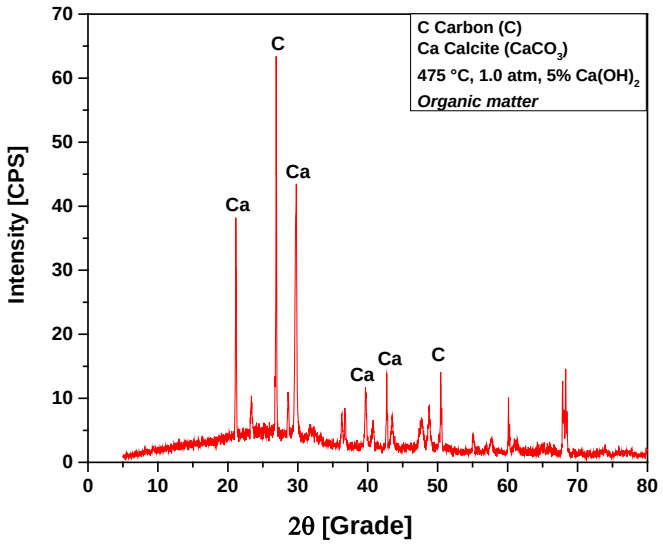

Figure 15. XRD of solid phase products by catalytic cracking of (organic matter + paper) fraction of MHSW at 475 °C, 1.0 atm, with 5.0% (wt.) $Ca(OH)_2$, using a borosilicate glass reactor of 125 mL, in laboratory scale.

The XRD analysis of bio-char obtained by catalytic cracking of (organic matter + paper) fraction of MHSW at 475 °C, 1.0 atmosphere, with 10% (wt.) $Ca(OH)_2$, shown in Figure 16, identified the presence of three crystalline phase, $CaCO_3$ (Calcite), graphite (C), and quartz (SiO_2). The occurrence of quartz (SiO_2) is probably due to presence of small particles of sand within OFMHSW. Four peaks are associated to the crystalline phase $CaCO_3$ (Calcite), one of high intensity on the position 2θ: 29.5 (100%), and three of low intensity on the positions 2θ: 20.9 (31.6%), 2θ: 36.6 (33.3%), and 2θ: 39.5 (16%). One peak of high intensity associated to the crystalline phase graphite (C) on the position 2θ: 26.8 (100%). One peak of medium intensity associated to the crystalline phase quartz (SiO_2)

Preprints (www.preprints.org) | NOT PEER-REVIEWED | Posted: 26 August 2022 doi:10.20944/preprints202208.0438.v1

on the position 2θ: 77.8 (56.8%). In addition, by analyzing the XRD, one observes the high intensity of $CaCO_3$ (Calcite) peaks, proving that higher $Ca(OH)_2$ content, leads to higher the intensity of $CaCO_3$ (Calcite) peaks. This causes a decrease on the carbonization degree, that is, the carbon content in bio-char, being according to the findings reported by *Kumagai et. al.* [50].

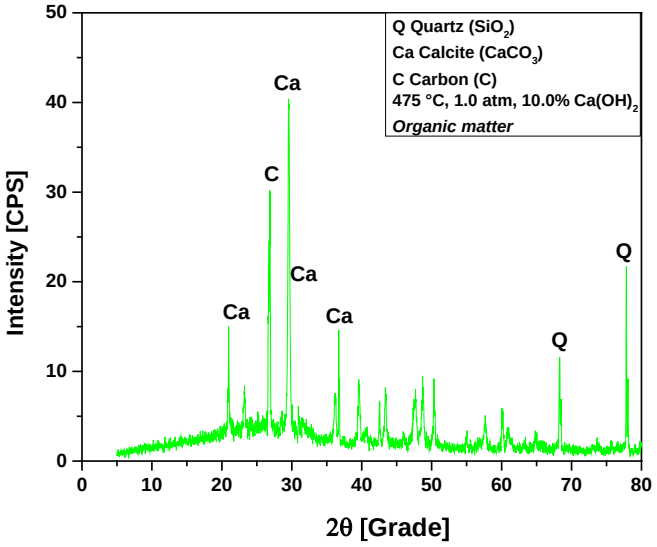

Figure 16. XRD of solid phase products by catalytic cracking of (organic matter + paper) fraction of MHSW at 475 °C, 1.0 atm, with 10.0% (wt.) $Ca(OH)_2$, using a borosilicate glass reactor of 125 mL, in laboratory scale.

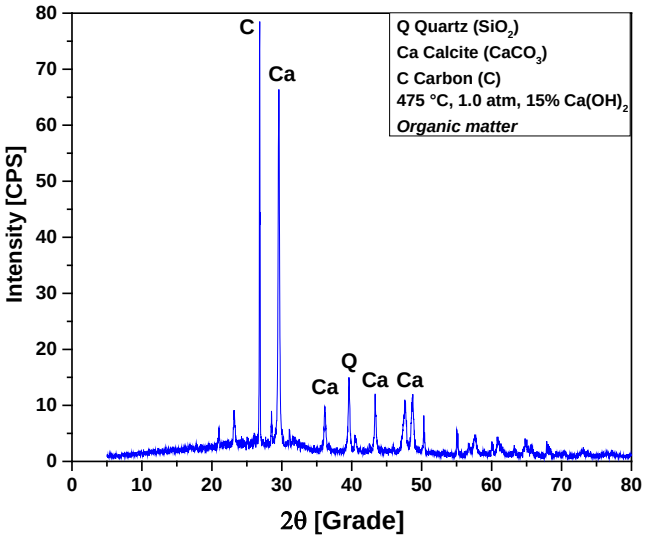

Figure 17. XRD of solid phase products by catalytic cracking of (organic matter + paper) fraction of MHSW at 475 °C, 1.0 atm, with 15.0% (wt.) $Ca(OH)_2$, using a borosilicate glass reactor of 125 mL, in laboratory scale.

The XRD analysis of bio-char obtained by catalytic cracking of (organic matter + paper) fraction of MHSW at 475 °C, 1.0 atmosphere, with 15% (wt.) $Ca(OH)_2$, shown in Figure 17, identified the presence of three crystalline phase, $CaCO_3$ (Calcite), graphite (C), and quartz (SiO_2). The occurrence of quartz (SiO_2) is probably due to presence of small particles of sand within OFMHSW. Three

peaks are associated to the crystalline phase $CaCO_3$ (Calcite), one of high intensity on the position 2θ: 29.5 (100%), and two of low intensity on the positions 2θ: 43.3 (12.1%) and 2θ: 36.1 (9%). One peak of high intensity associated to the crystalline phase graphite (C) on the position 2θ: 26.8 (100%). One peak of low intensity associated to the crystalline phase quartz (SiO_2) on the position 2θ: 39.6 (30%).

3.3. Gravimetric analysis of municipal household solid waste (MHSW)

3.3.1 *Route number, date, collecting time, mass of MHSW, percentage of class of materials*

Table 6 shows the results of gravimetric analysis of MHSW in the city of Belém-Pará-Brazil in the period from 18/10/2021 to 29/10/2021, according to ABNT NBR 1007 [58]. In addition, Table 1 includes the route number, date, collecting time, mass of MHSW, and percentage of MHSW fractions (metal, glass, polymers, *carbohydrates + lipids + proteins + fibers = organic matter*, textiles, *aluminum foil + plastic layers + cardboard + plastic caps + bioplastics = tetra pack*, paper, cardboard, *paper tissue + masks + disposal diapers + pads = sanitary household waste*). By analyzing the data in Table 6, one observes the heterogeneity of MHSW and hence, the difference on percentage of the different MHSW fractions on different days of collection. As for the variance in mass (wt.%) of each MHSW fraction, the organic matter fraction was higher compared to the other MHSW fractions, as it composes more than half of all other MHSW fractions for all the samples, and the percentage in weight varies between 54.44 and 71.91% (wt.). In the first sampling, it was obtained 54.44% (wt.), in the second 65.84% (wt.), in the third and fourth samples with 58.73% and 71.91% (wt.), respectively. By comparing the results illustrated in Table 6, for the organic fraction of MHSW, with similar data reported in the literature [53-55, 30, 56-57], described in Table 7, one observes that the variance in mass (wt.%) for organic fraction of municipal household solid waste is according to those reported in the literature [54-57]. In addition, the variance in mass (wt.%) for organic fraction of municipal household solid waste, *between 56.21 and 67.45% (wt.)*, lies between the interval of 56% (wt.) and 64% (wt.) of OFMHSW for middle and low income countries [62], which is the case of population income stratus of the neighborhoods of *Cremação* and *Guamá* in the city of Belém-Pará-Brazil.

Table 6. Gravimetric analysis of Municipal Household Solid Waste (MHSW) in the city of Belém-Pará-Brazil on 18/10/2021, 20/10/2021, 27/10/2021, and 29/10/2021 according to ABNT NBR 1007 [58], route number, date, collecting time, mass of MSW, percentage of class of materials (metal, glass, polymers, *carbohydrates + lipids + proteins + fibers = organic matter*, textiles, *aluminum foil + plastic layers + cardboard + plastic caps + bioplastics = tetra pack*, paper, cardboard, *paper tissue + masks + disposal diapers + pads = sanitary household waste*).

Route:	**1202**		**1202**		**1202**		**1202**			
Date:	**18/10/2021**	**Time**	**20/10/2021**	**Time**	**27/10/2021**	**Time**	**29/10/2021**	**Time**		
Mass of MHSW	**102.00**	**07:30**	**106.50**	**07:30**	**107.25**	**07:30**	**113.50**	**07:30**		
Class of MHSW	**Mass (kg)**	**(wt.%)**	**Mass (kg)**	**(wt.%)**	**Mass (kg)**	**(wt.%)**	**Mass (kg)**	**(wt.%)**	***Mean* (wt.%)**	***Deviation* (wt.%)**
Paper	1.00	0.98	2.70	2.54	4.70	4.40	3.70	3.27	2.80	±1.24
Cardboard	2.05	2.01	2.60	2.45	3.60	3.37	2.90	2.56	2.60	±0.49
Tetra Pak	1.10	1.08	1.10	1.04	2.05	1.92	0.30	0.26	1.08	±0.59
Hard Plastic	4.75	4.66	10.25	9.65	2.40	2.25	7.95	6.76	5.83	±2.72
Soft Plastic	9.65	9.47	4.30	4.05	5.90	5.53	11.15	9.85	7.23	±2.49
Metal	4.80	4.71	1.75	1.65	5.50	5.16	1.60	1.41	3.23	±1.71
Organic Matter	55.50	54.44	69.95	65.84	62.40	58.50	76.40	68.52	61.83	±5.62
Glass	9.80	9.61	1.60	1.51	1.90	1.78	0.35	0.33	3.31	±3.68
Inert	13.30	13.05	12.00	11.29	18.20	17.06	8.80	7,77	12.29	±3.35
Total	101.95	100.00	106.25	100.00	106.65	100.0	113.15	100.00		

 doi:10.20944/preprints202208.0438.v1

Table 7. Gravimetric analysis of Municipal Household Solid Waste (MHSW) reported in the literature [53-55, 30, 56-57], percentage of class of materials (metal, steel, aluminum, glass, sand, *plastic films + rigid plastics = polymers/plastics*, *carbohydrates + lipids + proteins + fibers = organic matter*, wood, textiles, rubber, leather, *aluminum foil + plastic layers + cardboard + plastic caps + bioplastics = tetrapak*, paper, cardboard, *paper tissue + masks + disposal diapers + pads = sanitary household waste, others*).

	[53]		[54]		[55]		[30]		[56]		[57]
MHSW		*MHSW*	(wt.%)	*MHSW*	(wt.%)	*MHSW*	(wt.%)	*MHSW*	(wt.%)	*MHSW*	(wt.%)
Food/Yard	38.79	Food	50.60	Garbage	68.67	Paper	5.45	Food	55.86	Metal	2.90
Sanitary/Diapers	10.80	Plastic	17.40	Plastic	11.45	Plastic	8.80	Wood	2.94	Steel	2.30
Plastic	14.77	Paper	12.00	Glass	1.41	Rubber	11.35	Paper	8.52	Aluminum	0.60
Paper	11.12	Cardboard	6.60	Paper/Cardboard	6.43	Textiles	5.45	Textiles	3.16	Paper/Cardboard/Tetrapak	13.10
Textile	8.94	Textile	1.93	Metals	2.71	Wood	25.29	Plastic	11.15	Plastic Film	8.90
Glass/Metal/Sand	15.58	Wood	2.00	Textile	1.50	Food	39.71	Rubber	0.84	Rigid Plastic	4.60
-		Leather	0.13	Others	7.83	Metal	0.10	Metal/Glass/Sand	18.36	Glass	2.40
-		Glass	2.90	-	-	Sand	3.85	-	-	Organic Matter	51.40
-		Metal	2.71	-	-	-	-	-	-	Others	16.70
-		Others	3.73	-	-	-	-	-	-	-	-
Total	100.00	Total	100.00	100.00	100.00	100.0	100.00	100.0	100.00	100.0	100.00

3.4. Pyrolysis of MHSW fraction (organic matter + paper) in fixed bed reactor

3.4.1 *Process conditions, mass balances, and yields of reaction products*

3.4.1.1 Influence of pyrolysis temperature

The process parameters, mass balances, and yields of reaction products (liquids, solids, H_2O, and gas) by pyrolysis of MHSW fraction (organic matter + paper) at 400, 450, and 475 °C, 1.0 atmosphere, in laboratory scale, is shown in Table 8. The pyrolysis experiments show bio-oil yields between 2.63 and 9.41% (wt.), aqueous phase yields between 28.58 and 35.08% (wt.), solid phase yields between 35.29 and 45.75% (wt.), and gas yields between 16.54 and 26.72% (wt.). The bio-oil yield increases with pyrolysis temperature, as more energy is available to promote the fragmentation of strong organic chemical bonds. Temperature has a great effect on the distribution of reaction products. The results show that highest bio-char yield of 45.75% (wt.) is obtained at 400°C, while the highest bio-oi and gas yields of 9.41% (wt.) and 26.72% (wt.), achieved at 475°C.

Table 8. Process parameters, mass balances, and yields of reaction products (liquids, solids, H_2O, and gas) by pyrolysis of MHSW fraction (organic matter + paper) at 400, 450, and 475 °C, 1.0 atm0sphere, in laboratory scale.

Process Parameters	0.0% (wt.)		
	400 °C	450 °C	475 °C
Mass of residual fat (g)	50.14	50.29	50.49
Cracking time (min)	70	100	70
Initial cracking temperature (°C)	397	348	318
Mechanical system stirring speed (rpm)	0	0	0
Mass of solid (Coke) (kg)	22.94	19.07	17.82
Mass of liquid (Bio-oil) (kg)	**1.32**	**3.74**	**4.75**
Mass of H_2O (kg)	17.59	17.10	14.43
Mass of gas (kg)	8.29	10.09	13.49
Yield of Bio-oil (wt.%)	**2.63**	**7.43**	**9.41**
Yield of H_2O (wt.%)	35.08	34.00	28.58
Yield of Coke (wt.%)	**45.75**	**37.92**	**35.29**
Yield of Gas (wt.%)	**16.54**	**20.65**	**26.72**

Preprints (www.preprints.org) | NOT PEER-REVIEWED | Posted: 26 August 2022 doi:10.20944/preprints202208.0438.v1

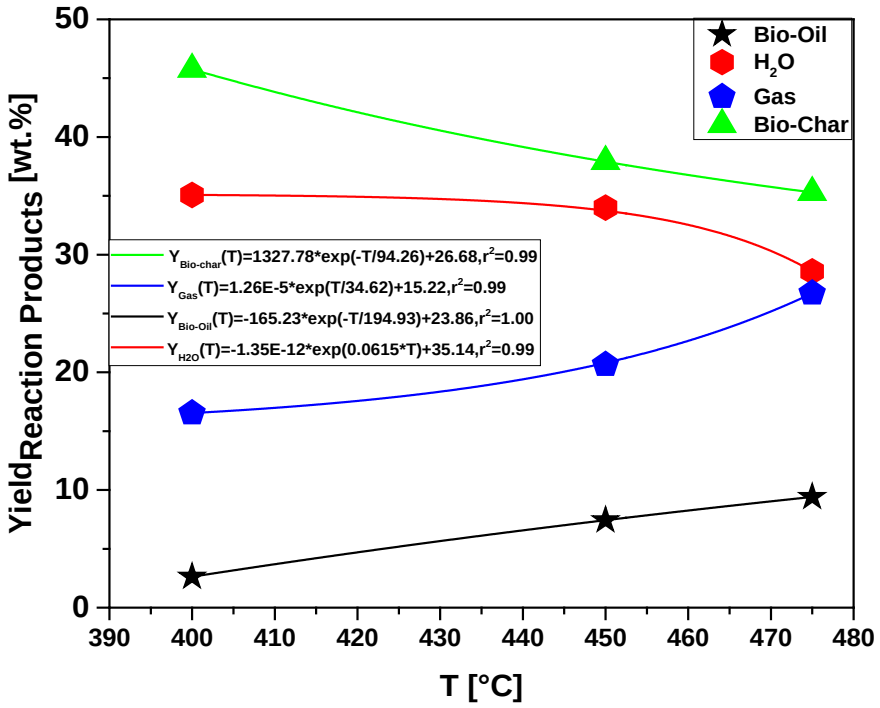

Figure 18. Effect of pyrolysis temperature on the yields of reaction products (liquids, solids, H_2O, and gas) by pyrolysis of MHSW fraction (organic matter + paper) at 400, 450, and 475 °C, 1.0 atmosphere, in laboratory scale.

The yield behavior of bio-oil is according to similar studies reported in the literature for pyrolysis of MSW [8, 12-13, 19, 23-24, 26-27, 31]. In all the studies, the yield of bio-oil increases with temperature between 350 and 600 °C, decreasing after 600 °C, while the of bio-char decreases [8, 12-13, 19, 23-24, 26-27, 31]. In addition, the yield of gas increases continuously [8, 12-13, 23-24, 26-27, 31]. *Song et. al.* [24], reported for the pyrolysis of MSW that the yield of bio-char increases between 400 and 600 °C, reaching a maximum at 600 °C, decreasing after 600 °C, while that of bio-char decreases almost exponentially, and the gas yield increases continuously, being according to the yields of reaction products as a function of temperature plotted in Figure 18.

3.4.1.2 Influence of catalyst-to-MHSW fraction

Table 9 illustrates the process parameters, mass balances, and yields of reaction products (liquids, solids, H_2O, and gas) by catalytic cracking of MHSW fraction (organic matter + paper) at 475 °C, 1.0 atmosphere, with 5.0, 10.0 and 15.0% (wt.) $Ca(OH)_2$ as catalyst, in laboratory scale. The catalytic cracking experiments show bio-oil yields between 5.52 and 7.0% (wt.), aqueous phase yields between 34.30 and 35.37% (wt.), solid phase yields between 30.40 and 35.27% (wt.), and gas yields between 23.82 and 27.37% (wt.). The bio-oil and gas yields increase slightly with CaO content, while that of bio-char decreases, and the H_2O phase remains constant, being according to the yields of reaction products as a function of CaO content plotted in Figure 19. The results is according to *Song et. al.* [24], who studied the catalytic cracking of MSW with CaO as catalyst, reporting that increasing the content of CaO between 0.0 and 7.0% (wt.), the yields of H_2O phase and bio-char remain constant, while that of gas increases slightly, and the yield of bio-oil decreases. In fact, according to *Kumagai et. al.* [50], calcium oxide (CaO) is transformed into calcite ($CaCO_3$) due to decarboxylation of

Preprints (www.preprints.org) | NOT PEER-REVIEWED | Posted: 26 August 2022 doi:10.20944/preprints202208.0438.v1

OFMHSW pyrolysis vapor compounds containing carboxyl groups, such as carboxylic acids, by CaO [50]. In this context, it is expected that bio-oils formed by catalytic cracking of OFMHSW using CaO as catalysts not only to be enriched in hydrocarbons but also contains lower acidity, as $CaCO_3$ is a stronger alkali compared to CaO.

Table 9. Process parameters, mass balances, and yields of reaction products (liquids, solids, H_2O, and gas) by thermal catalytic cracking of MHSW fraction (organic matter + paper) at 475 °C, 1.0 atm, 5.0, 10.0, and 15.0% (wt.) $Ca(OH)_2$, in laboratory scale.

Process Parameters	475 (°C)			
	0.0 (wt.)	5.0 (wt.)	10.0 (wt.)	15.0 (wt.)
Mass of OFMHSW (g)	50.49	40.0	40.0	40.0
Cracking time (min)	70	75	70	70
Initial cracking temperature (°C)	318	220	206	268
Mechanical system stirring speed (rpm)	0	0	0	0
Mass of solid (Coke) (kg)	17.82	14.11	13.56	12.16
Mass of liquid (Bio-oil) (kg)	**4.75**	**2.21**	**2.27**	**3.16**
Mass of H_2O (kg)	14.43	14.15	13.72	13.73
Mass of gas (kg)	13.49	9.53	10.45	10.95
Yield of Bio-oil (wt.%)	**9.41**	5.52	5.67	7.90
Yield of H_2O (wt.%)	28.58	35.37	34.30	34.32
Yield of Coke (wt.%)	**35.29**	35.27	33.90	30.40
Yield of Gas (wt.%)	**26.72**	23.82	26.12	27.37

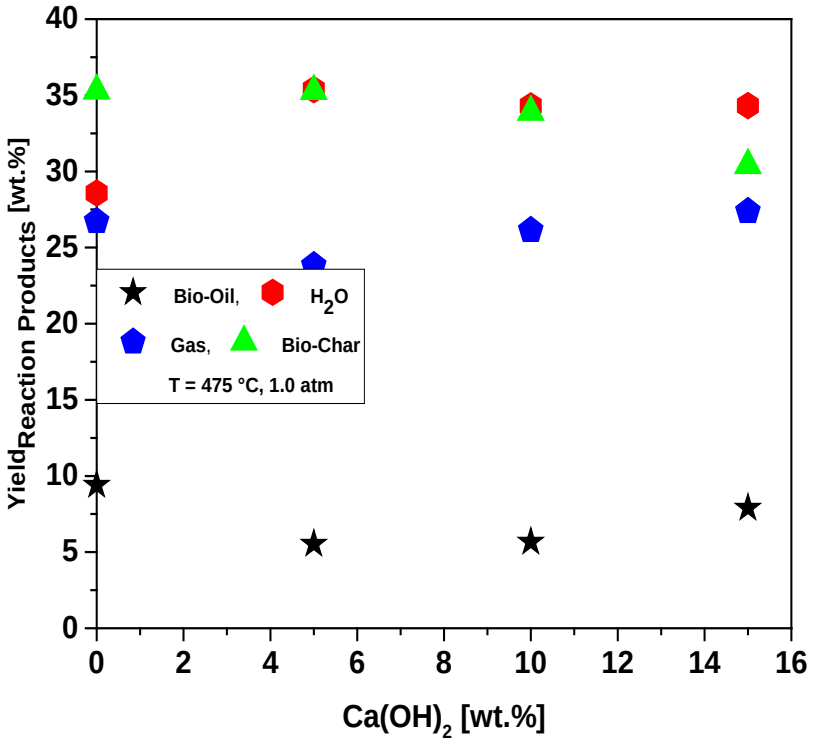

Figure 19. Effect of $Ca(OH)_2$-to-MHSW ratio on the yield of bio-oil, bio-char, aqueous, and gas phases by thermal catalytic cracking of MHSW fraction (organic matter + paper) at 475 °C, 1.0 atm, 5.0, 10.0, and 15.0% (wt.) $Ca(OH)_2$, in laboratory scale.

3.4.2 *Physicochemical and compositional characterization of bio-oil*

 doi:10.20944/preprints202208.0438.v1

3.4.2.1 Acidity of bio-oil

Table 10 shows the effect of temperature on the acidity of bio-oil by pyrolysis of MHSW fraction (organic matter + paper) at 400, 450, and 475 °C, 1.0 atm, in laboratory scale. The acidity of bio-oil decreases with increasing process temperature, while that of aqueous phase increases. The acidity of bio-oil obtained at 475 °C, 1.0 atm, in laboratory scale is close to that of bio-oil (70.25 ± 1.0 mg KOH/g) obtained by pyrolysis of açaí (*Euterpe oleraceae*, Mart) seeds at 450 °C, 1.0 atm, in laboratory scale. As described in section 3.2.3, higher temperatures promotes the formation calcite ($CaCO_3$), a strong alkali, by carbonation of calcium oxide (CaO) with CO_2 at high temperatures [60], as well as by decarboxylation of OFMHSW pyrolysis vapor compounds containing carboxyl groups, such as carboxylic acids, by CaO [50], and decarboxylation of carboxylic acids produces bio-oils with lower acidity.

Table 10. Effect of temperature on the acid index of bio-oils and aqueous phase by pyrolysis of MHSW fraction (organic matter + paper) at 400, 450, and 475 °C, 1.0 atm, in laboratory scale.

Physicochemical Property	**Temperature**		
Acid Index	400 °C	450 °C	475 °C
$I.A_{Bio\text{-}Oil}$ [mg KOH/g]	113.15	97.78	71.24
$I.A_{Aqueous\ Phase}$ [mg KOH/g]	45.55	53.88	67.05

Table 10 shows the effect of $Ca(OH)_2$ content on the acidity of bio-oil by catalytic cracking of MHSW fraction (organic matter + paper) at 475 °C, 1.0 atm, with 5.0, 10.0, and 15.0% (wt.) $Ca(OH)_2$, in laboratory scale. The addition of $Ca(OH)_2$ causes a drastic diminution on the acidity of bio-oil, as calcite is a strong alkali. However, by increasing the $Ca(OH)_2$ content, the acidity of both bio-oil and aqueous phase remain almost constant., that is, $Ca(OH)_2$ content has little or almost no effect on the acidity of bio-oils. This is probably due to the reaction mechanism of decarboxylation [62]. If the reaction mechanism produces H^+ as intermediate, an increase on the $Ca(OH)_2$-to-MHSW fraction ratio, that is, an increase on the concentration of alkalis has a limited effect [62].

Table 11. Effect of $Ca(OH)_2$ content on the acid index of bio-oils and aqueous phase by catalytic cracking of MHSW fraction (organic matter + paper) at 475 °C, 1.0 atm, 5.0, 10.0, and 15.0% (wt.) $Ca(OH)_2$, in laboratory scale.

Physicochemical Property	475 °C		
	$Ca(OH)_2$		
Acid Index	5.0% (wt.)	10.0% (wt.)	15.0% (wt.)
$I.A_{Bio\text{-}Oil}$ [mg KOH/g]	36.26	34.43	37.52
$I.A_{Aqueous\ Phase}$ [mg KOH/g]	43.56	43.42	43.42

3.4.2.2 FT-IR of bio-oil

The FT-IR qualitative analysis of chemical functions present in the bio-oils obtained by pyrolysis of MHSW fraction (organic matter + paper) at 400, 450, and 475 °C, 1.0 atm, in laboratory scale, is shown in Figure 20. A wide vibration band between 3600–3200 cm^{-1} is observed, characteristic of the O–H angular deformation, associated to the presence of H_2O. The bands close to 2922 and 2854 cm^{-1} refer to the aliphatic axial deformations of the C-H bonds of the methylene (CH_2) and methyl (CH_3) groups. The peak of 1707 cm^{-1} indicates the presence of carbonyls of oxygenated compounds. The 1456 cm^{-1} band can be attributed to CH_2 bond stretches and the 1377 cm^{-1} band is attributed to CH_3 (methyl) stretches. The peak of asymmetric angular strain outside the plane of the C-H bond of the methylene group is observed at 725 cm^{-1}.

Preprints (www.preprints.org) | NOT PEER-REVIEWED | Posted: 26 August 2022 doi:10.20944/preprints202208.0438.v1

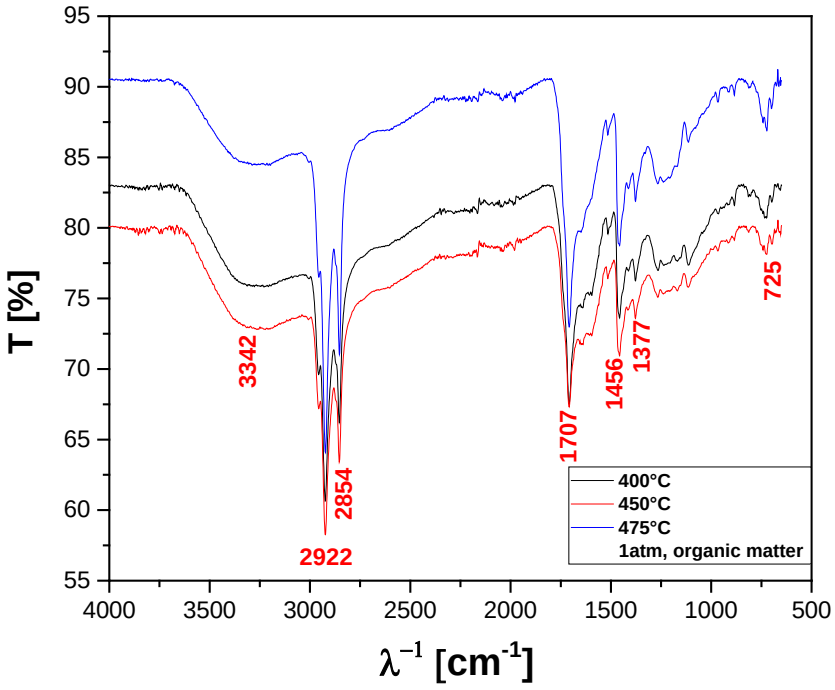

Figure 20. FT-IR of bio-oil obtained by pyrolysis of MHSW fraction (organic matter + paper) at 400, 450, and 475 °C, 1.0 atmosphere, in laboratory scale.

The FT-IR qualitative analysis of chemical functions present in the bio-oils obtained by catalytic cracking of MHSW fraction (organic matter + paper) at 475 °C, 1.0 atm, 5.0, 10.0, and 15.0% (wt.) $Ca(OH)_2$, in laboratory scale, is shown in Figure 21.

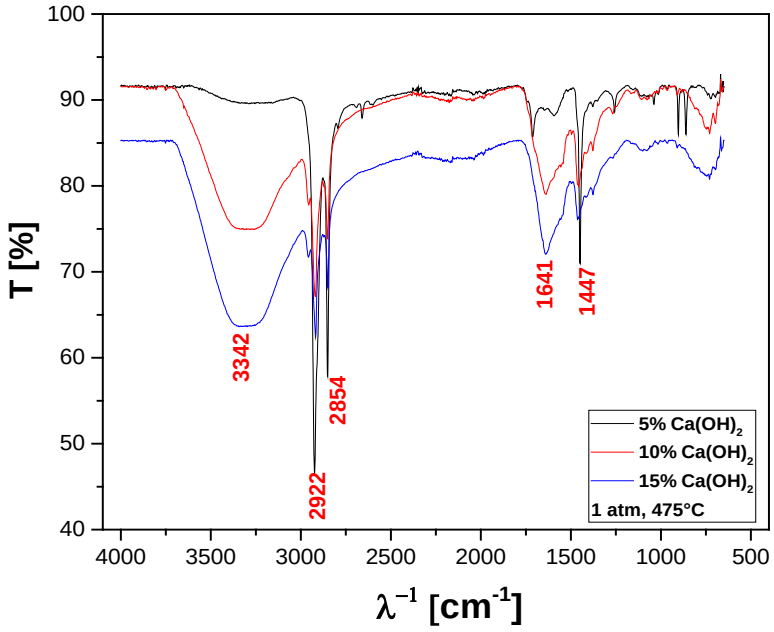

Figure 21. FT-IR of bio-oil obtained by catalytic cracking of MHSW fraction (organic matter + paper) at 475 °C, 1.0 atm, 5.0, 10.0, and 15.0% (wt.) $Ca(OH)_2$, in laboratory scale.

Preprints (www.preprints.org) | NOT PEER-REVIEWED | Posted: 26 August 2022 doi:10.20944/preprints202208.0438.v1

It is observed a wide vibration band between 3600–3200 cm^{-1}, characteristic of the O–H angular deformation, associated to the presence of H_2O. The bands close to 2922 and 2854 cm^{-1} refer to the aliphatic axial deformations of the C-H bonds of the methylene (CH_2) and methyl (CH_3) groups. It can also be observed, a stretch that occurs at 1660–1600 cm^{-1}, the conjugation moves the C = C stretch to lower frequencies and increases the intensity. The band of 1447 cm^{-1} can be attributed to the stretching of CH_2 bonds. The FT-IT is characteristic of aliphatic hydrocarbons as well as oxygenates, associated to the presence of a carboxyl group, characteristics of carboxylic acids.

3.4.2.3 Chemical composition of bio-oil

Table 12 and Figures 22 show the effect of temperature on the content of hydrocarbons and oxygenates in bio-oil obtained by pyrolysis of MHSW fraction (organic matter + paper) at 400, 450, and 475 °C, 1.0 atmosphere, in laboratory scale. The chemical functions (alkanes, alkenes, alkynes, aromatics, carboxylic acids, esters, alcohols, phenols, amines, amides, aldehydes, nitrogenates, and ketones), sum of peak areas, CAS numbers, and retention times of all the molecules identified in bio-oil by GC-MS, are illustrated in Supplementary Tables S1-S3. The concentration of hydrocarbons in bio-oil has a maximum at 450 °C. This is according to the acidity of bio-oils illustrated in Table 11, where the bio-oil obtained by catalytic cracking of MHSW fraction (organic matter + paper) at 475 °C, 1.0 atm, 10.0% (wt.) $Ca(OH)_2$ presents its lower acid value.

Table 12. Effect of temperature on the chemical composition, expressed as hydrocarbons and oxygenates/nitrogenates, of bio-oils obtained by pyrolysis of MHSW fraction (organic matter + paper) at 400, 450, and 475 °C, 1.0 atm, in laboratory scale.

Temperature [°C]	Concentration [%area.]	
	Hydrocarbons	Oxygenates/Nitrogenates
400	23.74	76.26
450	37.54	62.50
475	20.81	79.81

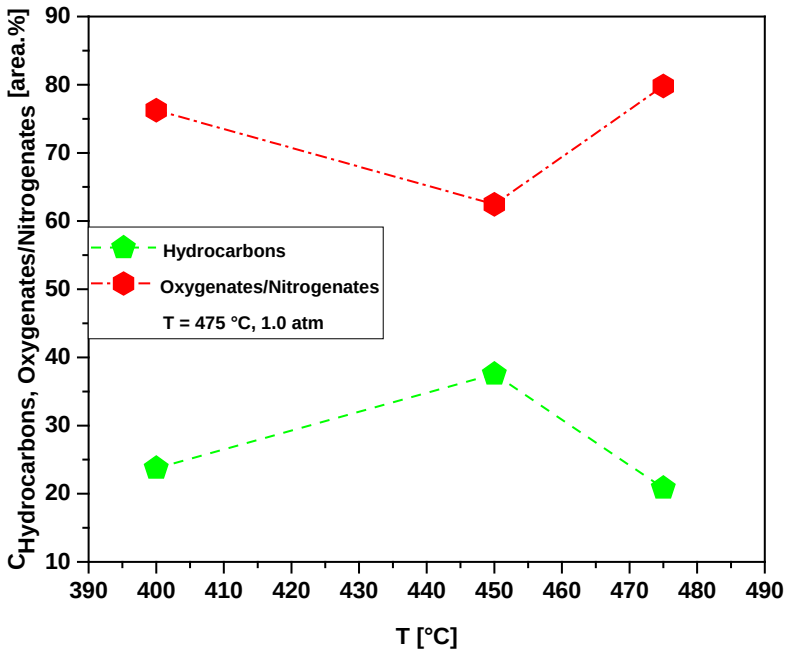

Figure 23. Effect of temperature on the chemical composition, expressed as hydrocarbons and oxygenates/nitrogenates, of bio-oils obtained by pyrolysis of MHSW fraction (organic matter + paper) at 400, 450, and 475 °C, 1.0 atm, in laboratory scale.

Preprints (www.preprints.org) | NOT PEER-REVIEWED | Posted: 26 August 2022 doi:10.20944/preprints202208.0438.v1

Figures 23 and Tables S4-S6 show the effect of $Ca(OH)_2$-to-MHSW fraction ratio on the content of hydrocarbons and oxygenates in bio-oil obtained by catalytic cracking of MHSW fraction (organic matter + paper) at 475 °C, 1.0 atm, 5.0, 10.0, and 15.0% (wt.) $Ca(OH)_2$, in laboratory scale. The chemical functions (alkanes, alkenes, alkynes, aromatics, esters, carboxylic acids, phenols, aldehydes, alcohols, amines, amides, nitrogenates, and ketones), sum of peak areas, CAS numbers, and retention times of all the molecules identified in bio-oil by GC-MS, are illustrated in Supplementary Tables S4-S4. The concentration of hydrocarbons in bio-oil increases exponentially with increasing $Ca(OH)_2$-to-MHSW fraction ratio due to the catalytic deoxygenation of fatty acids molecules, by means of de-carboxylation/de-carbonylation, producing aliphatic and aromatic hydrocarbons, as reported in the literature [45], while that of oxygenates decreases exponentially. The bio-oils compositions described in Tables S1-S6 are according to those described in the literature for bio-oils obtained by pyrolysis of MHSW [8, 11-12, 17, 19, 21-24, 26, 28]. The occurrence of compounds containing nitrogen is due probably to the presence of nitrogen in OFMHSW determined by elemental analysis as reported by *AlDayyat et. al.* [20], and by *Ghavanati et. al.* [59].

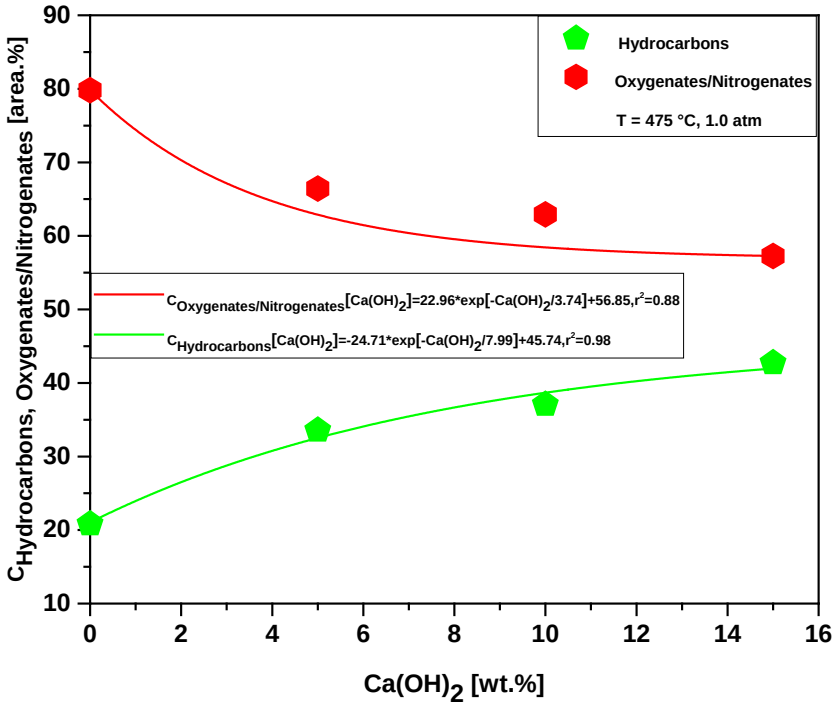

Figure 23. Effect of $Ca(OH)_2$-to-MHSW ratio on the content of oxygenates and hydrocarbons in bio-oil obtained by catalytic cracking of MHSW fraction (organic matter + paper) at 475 °C, 1.0 atm, 5.0, 10.0, and 15.0% (wt.) $Ca(OH)_2$, in laboratory scale.

5. Conclusions

The pyrolysis of MHSW fraction (organic matter + paper) produces a bio-oil with yields between 2.63 and 9.41% (wt.).

The bio-oil yield increases with pyrolysis temperature. For the catalytic cracking, the bio-oil and gas yields increase slightly with CaO content, while that of bio-char decreases, and the H_2O phase remains constant.

The acidity of bio-oil decreases with increasing process temperature and with aid $Ca(OH)_2$ as catalyst.

The concentration of hydrocarbons in bio-oil increases with increasing $Ca(OH)_2$-to-MHSW fraction ratio due to the catalytic deoxygenation of fatty acids molecules, by means of de-carboxylation/de-carbonylation, producing aliphatic and aromatic hydrocarbons.

Supplementary Materials: The following are available. Table S1: Classes of compounds, summation of peak areas, CAS number, and retention times of chemical compounds identified by CG-MS in bio-oil by pyrolysis of (organic matter + paper) fraction from MHSW at 400 °C, 1.0 atm, in laboratory scale. Table S2: Classes of compounds, summation of peak areas, CAS number, and retention times of chemical compounds identified by CG-MS in bio-oil by pyrolysis of (organic matter + paper) fraction from MHSW at 450 °C, 1.0 atm, in laboratory scale. Table S3: Classes of compounds, summation of peak areas, CAS number, and retention times of chemical compounds identified by CG-MS in bio-oil by pyrolysis of (organic matter + paper) fraction from MHSW at 475 °C, 1.0 atm, in laboratory scale. Table S4: Classes of compounds, summation of peak areas, CAS number, and retention times of chemical compounds identified by CG-MS in bio-oil by thermal catalytic cracking of (organic matter + paper) fraction from MHSW at 475 °C, 1.0 atm, 5.0% (wt.) of Ca(OH) 2 , in laboratory scale. Table S5: Classes of compounds, summation of peak areas, CAS number, and retention times of chemical compounds identified by CG-MS in bio-oil by thermal catalytic cracking of (organic matter + paper) fraction from MHSW at 475 °C, 1.0 atm, 10.0% (wt.) of Ca(OH) 2 , in laboratory scale. Table S6: Classes of compounds, summation of peak areas, CAS number, and retention times of chemical compounds identified by CG-MS in bio-oil by thermal catalytic cracking of (organic matter + paper) fraction from MHSW at 475 °C, 1.0 atm, 5.0% (wt.) of Ca(OH) 2 , in laboratory scale.

Author Contributions: The individual contributions of all the co-authors are provided as follows: F.P.d.C.A. contributed with formal analysis and writing original draft preparation, investigation and methodology, D.O.P. contributed with formal analysis, investigation and methodology, J.C.C.d.S. contributed with formal analysis, investigation and methodology, J.F.H.F. contributed with formal analysis, investigation and methodology, K.C.A.B. contributed with investigation and methodology, L.P.B. contributed with investigation and methodology, C.C.F. contributed with investigation and methodology, A.F.d.F.C. contributed with investigation and methodology, L.M.P. contributed with investigation and methodology, S.P.A.d.P. contributed with resources, chemical analysis R.B.P.F. contributed with collecting and sampling, B.R.C. contributed with collecting and sampling, Y.S.C. contributed with chemical analysis, A.C.P.A. contributed with SIG analysis, D.A.R.d.C. contributed with investigation and methodology, M.C.S. contributed with formal analysis, investigation and methodology, N.M.M. contributed with formal analysis, investigation and methodology, S.D.J. contributed with resources, chemical analysis, A.A.M.P.J. contributed with chemical analysis and formal analysis, L.E.P.B. with co-supervision, and resources, J.A.R.P. contributed with supervision, conceptualization, and data curation, and N.T.M. contributed with supervision, conceptualization, and data curation. All authors have read and agreed to the published version of the manuscript.

Funding: This research received no external funding.

Institutional Review Board Statement: Not applicable.

Informed Consent Statement: Not applicable.

Acknowledgments: I would like to acknowledge and dedicate this research in memory to Hélio da Silva Almeida, he used to work at the Faculty of Sanitary and Environmental Engineering/UFPa, and passed away on 13 March 2021. His contagious joy, dedication, intelligence, honesty, seriousness, and kindness will always be remembered in our hearts.

Conflicts of Interest: The authors declare no conflict of interest.

References

1. Shamim Mia, Md. Ektear Uddin, Md. Abdul Kader, Amimul Ahsan, M.A. Mannan, Mohammad Monjur Hossain, Zakaria M. Solaiman. Pyrolysis and co-composting of municipal organic waste in Bangladesh: A quantitative estimate of recyclable nutrients, greenhouse gas emissions, and economic benefits. Waste Management 75 (2018) 503–513
2. Juan Galvarino Cerda Balcazar, Rubens Alves Dias, José Antonio Perrella Balestier. Analysis of hybrid waste-to-energy for medium-sized cities. Energy 55 (2013) 728-741
3. Vaibhav Srivastava, Sultan Ahmed Ismail, Pooja Singh, Rajeev Pratap Singh. Urban solid waste management in the developing world with emphasis on India: challenges and opportunities. Rev Environ Sci Biotechnol (2015) 14:317–337
4. Christian Riuji Lohri, Hassan Mtoro Rajabu, Daniel J. Sweeney, Christian Zurbrügg. Char fuel production in developing countries – A review of urban biowaste carbonization. Renewable and Sustainable Energy Reviews 59 (2016) 1514–1530
5. Christian Riuji Lohri, Adam Faraji, Elia Ephata, Hassan Mtoro Rajabu, Christian Zurbrügg. Urban biowaste for solid fuel production: Waste suitability assessment and experimental carbonization in Dar es Salaam, Tanzania. Waste Management & Research 2015, Vol. 33(2) 175–182
6. Christian Riuji Lohri, Stefan Diener, Imanol Zabaleta, Adeline Mertenat, Christian Zurbrügg. Treatment technologies for urban solid biowaste to create value products: a review with focus on low- and middle income settings. Rev Environ Sci Biotechnol (2017) 16:81–130 DOI 10.1007/s11157-017-9422-5
7. Yin Ding, Jun Zhao, Jia-Wei Liu, Jizhi Zhou, Liang Cheng, Jia Zhao, Zhe Shao, Çagatay Iris, Bingjun Pan, Xiaonian Li, Zhong-Ting Hu. A review of China's municipal solid waste (MSW) and comparison with international regions: Management and technologies in treatment and resource utilization. Journal of Cleaner Production 293 (2021) 126144
8. Douglas Alberto Rocha de Castro, Haroldo Jorge da Silva Ribeiro, Lauro Henrique Hamoy Guerreiro, Lucas Pinto Bernar, Sami Jonatan Bremer, Marcelo Costa Santo, Hélio da Silva Almeida, Sergio Duvoisin, Jr., Luiz Eduardo Pizarro Borges and Nélio Teixeira Machado. Production of Fuel-Like Fractions by Fractional Distillation of Bio-Oil from Açaí (Euterpe oleracea Mart.) Seeds Pyrolysis. Energies 2021, 14, 3713. https://doi.org/10.3390/en14133713
9. Paulo Bisi dos Santos, Jr., Haroldo Jorge da Silva Ribeiro, Armando Costa Ferreira, Caio Campos Ferreira, Lucas Pinto Bernar, Fernanda Paula da Costa Assunção, Douglas Alberto Rocha de Castro, Marcelo Costa Santos, Sergio Duvoisin, Jr., Luiz Eduardo Pizarro Borges and Nélio Teixeira Machado. Process Analysis of PMMA-Based Dental Resins Residues Depolymerization: Optimization of Reaction Time and Temperature. Energies 2022, 15, 91. https://doi.org/10.3390/en15010091
10. Taihana Parente Paula, Maria F. Vieira Marques, Mônica Regina da Costa Marques. Influence of mesoporous structure ZSM-5 zeolite on the degradation of Urban plastics waste. Journal of Thermal Analysis and Calorimetry (2019) 138:3689–3699 https://doi.org/10.1007/s10973-019-08907-0
11. L. Quesada, M. Calero, M.A. Martín-Lara, A. Perez, G. Blázquez. Characterization of fuel produced by pyrolysis of plastic film obtained of municipal solid waste. Energy 186 (2019) 115874
12. Anh N. Phan, Changkook Ryu, Vida N. Sharifi, Jim Swithenbank. Characterisation of slow pyrolysis products from segregated wastes for energy production. J. Anal. Appl. Pyrolysis 81 (2008) 65–71
13. Yao Bin Yang, Anh N Phan, Changkook Ryu, Vida Sharifi, Jim Swithenbank. Mathematical modelling of slow pyrolysis of segregated solid wastes in a packed-bed pyrolyser. Fuel 86 (2007) 169–180
14. L. Sørum, M.G. Grønli, J.E. Hustad. Pyrolysis characteristics and kinetics of municipal solid wastes. Fuel 80 (2001) 1217-1227
15. Honghong Shi, Nader Mahinpey, Aqsha, Rico Silbermann. Characterization, thermochemical conversion studies, and heating value modeling of municipal solid waste. Waste Management 48 (2016) 34–47
16. S. Vakalis, A. Sotiropoulos, K. Moustakas, D. Malamis, K. Vekkos, M. Baratieri. Thermochemical valorization and characterization of household biowaste. Journal of Environmental Management 203 (2017) 648e654
17. Chuan Peng, Wei Feng, Yanhui Zhang, Shifeng Guo, Zhile Yang, Xiangmin Liu, Tengfei Wang, Yunbo Zhai. Low temperature co-pyrolysis of food waste with PVC-derived char: Products distributions, char properties and mechanism of bio-oil upgrading. Energy 219 (2021) 119670
18. Obid Tursunov. A comparison of catalysts zeolite and calcined dolomite for gas production from pyrolysis of municipal solid waste (MSW). Ecological Engineering 69 (2014) 237–243 (17)
19. Muhammad Saiful Islam, M. Yunus Miah, Mohammad Ismail, Mohammad Shah Jamal, Sujit Kumar Banik and Manoranjan Saha. Production of Bio-Oil from Municipal Solid Waste by Pyrolysis. Bangladesh J. Sci. Ind. Res. 45(2), 91-94, 2010
20. Ebtihal A. AlDayyat, Motasem N. Saidan, Zayed Al-Hamamre, Mohammad Al-Addous, Malek Alkasrawi. Pyrolysis of Solid Waste for Bio-Oil and Char Production in Refugees' Camp: A Case Study. Energies 2021, 14, 3861
21. I M Gandidi, M D Susila, N A Pambudi. Co-cracking of real MSW into bio-oil over natural kaolin. Earth and Environmental Science 60 (2017) 012019
22. I M Gandidi, M D Susila, H Rustamaji. Effect of natural zeolite and kaolin as a catalyst in the isothermal-catalytic cracking of real municipal solid waste (MSW) for bio-oil production. Earth and Environmental Science 160 (2018) 012018

23. I. Velghe, R. Carleer, J. Yperman, S. Schreurs. Study of the pyrolysis of municipal solid waste for the production of valuable products. Journal of Analytical and Applied Pyrolysis 92 (2011) 366–375
24. Qiang Song, Hong-yu Zhao, Wen-long Xing, Li-hua Song, Li Yang, Di Yang, Xinqian Shu. Effects of various additives on the pyrolysis characteristics of municipal solid waste. Waste Management 78 (2018) 621–629
25. M.M. Hasan, M.G. Rasul, M.M.K. Khan, N. Ashwath, M.I. Jahirul. Energy recovery from municipal solid waste using pyrolysis technology: A review on current status and developments. Renewable and Sustainable Energy Reviews 145 (2021) 111073
26. Funda Ates, Norbert Miskolczi, Nikolett Borsodi. Comparision of real waste (MSW and MPW) pyrolysis in batch reactor over different catalysts. Part I: Product yields, gas and pyrolysis oil properties. Bioresource Technology 133 (2013) 443–454
27. Norbert Miskolczi, Funda Ates, Nikolett Borsodi. Comparison of real waste (MSW and MPW) pyrolysis in batch reactor over different catalysts. Part II: Contaminants, char and pyrolysis oil properties. Bioresource Technology 144 (2013) 370–379
28. Chong Chen, Yuqi Jin, Yong Chi. Effects of moisture content and CaO on municipal solid waste pyrolysis in a fixed bed reactor. Journal of Analytical and Applied Pyrolysis 110 (2014) 108–112
29. Qiang Song, Hong-yu Zhao, Wen-long Xing, Li-hua Song, Li Yang, Di Yang, Xinqian Shu. Effects of various additives on the pyrolysis characteristics of municipal solid waste. Waste Management 78 (2018) 621–629
30. Guicai Liu, Yanfen Liao, Shaode Guo, Xiaoqian Ma, Chengcai Zeng, Jie Wu. Thermal behavior and kinetics of municipal solid waste during pyrolysis and combustion process. Applied Thermal Engineering 98 (2016) 400–408
31. Alberto Veses, Olga Sanahuja-Parejo, María Soledad Callén, Ramón Murillo, Tomás García. A combined two-stage process of pyrolysis and catalytic cracking of municipal solid waste for the production of syngas and solid refusederived fuels. Waste Management 101 (2020) 171–179
32. Dezhen Chen, Lijie Yin, Huan Wang, Pinjing He. Pyrolysis technologies for municipal solid waste: A review. Waste Management 34 (2014) 2466–2486
33. Ayesha Tariq Sipra, Ningbo Gao, Haris Sarwar. Municipal solid waste (MSW) pyrolysis for bio-fuel production: A review of effects of MSW components and catalysts. Fuel Processing Technology 175 (2018) 131–147
34. Jia-Shun Lu, Yingju Chang, Chi-Sun Poon, Duu-Jong Lee. Slow pyrolysis of municipal solid waste (MSW): A review. Bioresource Technology 312 (2020) 123615
35. IBGE. Instituto Brasileiro de Geografia e Estatística. Censo Brasileiro de 2010. Rio de Janeiro: IBGE, 2012 https://censo2010.ibge.gov.br/
36. Nunes. L. R. S. Caracterização Física de Resíduos Sólidos no Porto de Belém e Terminal Petroquímico de Miramar. Dissertação (Mestrado em Engenharia Civil) - Universidade Federal do Pará, Instituto de Tecnologia, 2015 https://ppgec.propesp.ufpa.br/ARQUIVOS/dissertacoes/2015/lailanunes.pdf
37. Samuel Nahom Fesseha and Fan Bin. The Assessment of Solid Waste Products Management in Ethiopians Municipal Urban Areas. Int. J. Soc. Sci. Manage. Vol-2, issue-2: 165-179 DOI: 10.3126/ijssm.v2i2.12468
38. de Andrade Cordeiro, M.; de Almeida, O.; de Castro, D.A.; da Silva Ribeiro, H.J.; Machado, N.T. Produção de Etanol através da Hidrólise Enzimática do Caroço de Açaí (*Euterpe oleracea*, Mart.). Rev. Bras. Energ. Renov. 2019, 8, 122–152
39. ABNT – ASSOCIAÇÃO BRASILEIRA DE NORMAS TÉCNICAS. NBR 10.007: Amostragem de Resíduos Sólidos. . Rio de Janeiro, 2004.
40. H. da Silva Almeida, O.A. Corrêa, C.C. Ferreira, H.J. Ribeiro, D.A.R. de Castro, M.S. Pereira, A. de Andrade Mâncio, M.C. Santos, S.A.P. da Mota, J.A. da Silva Souza, Luiz E.P. Borges, N.M. Mendonça, N.T. Machado. Diesel-like hydrocarbon fuels by catalytic cracking of fat, oils, and grease (FOG) from grease traps. Journal of the Energy Institute 90 (2017) 337-354
41. H. da Silva Almeida, O.A. Corrêa, J.G. Eida, H.J. Ribeiro, D.A.R. de Castro, M.S. Pereira, L.M. Pereira, A. de Andrade Mâncio, M.C. Santos, S.A.P da Mota, J.A. da Silva Souza, Luiz E.P. Borges, N.M. Mendonça, N.T. Machado. Performance of thermochemical conversion of fat, oils, and grease into kerosene-like hydrocarbons in different production scales. Journal of Analytical and Applied Pyrolysis 120 (2016) 126–143
42. da Mota, S.A.; Mancio, A.A.; Lhamas, D.E.; de Abreu, D.H.; da Silva, M.S.; dos Santos, W.G.; de Castro, D.A.; de Oliveira, R.M.; Araújo, M.E.; Borges, L.E.; et al. Production of green diesel by thermal catalytic cracking of crude palm oil (Elaeis guineensis Jacq) in a pilot plant. J. Anal. Appl. Pyrolysis 2014, 110, 1–11
43. Ferreira, C.C.; Costa, E.C.; de Castro, D.A.; Pereira, M.S.; Mâncio, A.A.; Santos, M.C.; Lhamas, D.E.; da Mota, S.A.; Leão, A.C.; Duvoisin, S., Jr.; et al. Deacidification of organic liquid products by fractional distillation in laboratory and pilot scales. J. Anal. Appl. Pyrolysis 2017, 127, 468–489
44. Lucas Pinto Bernar, Caio Campos Ferreira, Augusto Fernando de Freitas Costa, Haroldo Jorge da Silva Ribeiro, Wenderson Gomes dos Santos, Lia Martins Pereira, Anderson Mathias Pereira, Nathalia Lobato Moraes, Fernanda Paula da Costa Assunção, Sílvio Alex Pereira da Mota, Douglas Alberto Rocha de Castro, Marcelo Costa Santos, Neyson Martins Mendonça, Sergio Duvoisin, Jr., Luiz Eduardo Pizarro Borges and Nélio Teixeira Machado. Catalytic Upgrading of Residual Fat Pyrolysis Vapors over Activated Carbon Pellets into Hydrocarbons-like Fuels in a Two-Stage Reactor: Analysis of Hydrocarbons Composition and Physical-Chemistry Properties. Energies 2022, 15, 4587. https://doi.org/10.3390/en15134587

45. Caio Campos Ferreira, Lucas Pinto Bernar, Augusto Fernando de Freitas Costa, Haroldo Jorge da Silva Ribeiro, Marcelo Costa Santos, Nathalia Lobato Moraes, Yasmin Santos Costa, Ana Cláudia Fonseca Baia, Neyson Martins Mendonça, Sílvio Alex Pereira da Mota, Fernanda Paula da Costa Assunção, Douglas Alberto Rocha de Castro, Carlos Castro Vieira Quaresma, Sergio Duvoisin, Jr., Luiz Eduardo Pizarro Borges and Nélio Teixeira Machado. Improving Fuel Properties and Hydrocarbon Content from Residual Fat Pyrolysis Vapors over Activated Red Mud Pellets in Two-Stage Reactor: Optimization of Reaction Time and Catalyst Content. Energies 2022, 15, 5595. https://doi.org/10.3390/en15155595
46. Hui Zhou, Yan Qiu Long, Ai Hong Meng, Qing Hai Li, Yan Guo Zhang. Classification of municipal solid waste components for thermal conversion in waste-to-energy research. Fuel 145 (2015) 151–157
47. M. Cabrera-Penna, J.E. Rodríguez-Páez. Calcium oxyhydroxide (CaO/Ca(OH)2) nanoparticles: Synthesis, characterization and evaluation of their capacity to degrade glyphosate-based herbicides (GBH). Advanced Powder Technology 32 (2021) 237–253
48. Ehsan Hassani, Farshad Feyzbar-Khalkhali-Nejad, Ali Rashti, and Tae-Sik Oh. Carbonation, Regeneration, and Cycle Stability of the Mechanically Activated Ca(OH)2 Sorbents for CO2 Capture: An In Situ X-ray Diffraction Study. : Ind. Eng. Chem. Res. 2020, 59, 11402−11411
49. Chitanya Gopu, Lihui Gao, Maurizio Volpe, Luca Fiori, Jillian L. Goldfarb. Valorizing municipal solid waste: Waste to energy and activated carbons for water treatment via pyrolysis. Journal of Analytical and Applied Pyrolysis 133 (2018) 48–58
50. Shogo Kumagai, Guido Grause, Tomohito Kameda, Toshiaki Yoshioka. Recovery of benzene-rich oil from the degradation of metal- and metal oxide-containing poly(ethylene terephthalate) composites. J Mater Cycles Waste Manag (2014) 16:282–290 DOI 10.1007/s10163-013-0194-x
51. Juan Antonio Madrida, Marcos Lanzón. Synthesis and morphological examination of high-purity Ca(OH)2 nanoparticles suitable to consolidate porous surfaces. Applied Surface Science 424 (2017) 2–8
52. Xiang Wang, Xiaoxiang Xu, Yu Ye, Chao Wang, Dan Liu, Xiaochao Shi, Sha Wang, Xi Zhu. In-situ High-Temperature XRD and FTIR for Calcite, Dolomite and Magnesite: Anharmonic Contribution to the Thermodynamic Properties. Journal of Earth Science, Vol. 30, No. 5, p. 964–976, October 2019, https://doi.org/10.1007/s12583-019-1236-7
53. Kelly C.R. Drudi, Ricardo Drudi, Gilberto Martins, Graziella Colato. Antonio, Juliana Tofano. C. Leite. Statistical model for heating value of municipal solid waste in Brazil based on gravimetric composition. Waste Management 87 (2019) 782–790
54. A.S. Nizami, K. Shahzad, M. Rehan, O.K.M. Ouda, M.Z. Khan, I.M.I. Ismail, T. Almeelbi, J.M. Basahi, A. Demirbas. Developing waste biorefinery in Makkah: A way forward to convert urban waste into renewable energy. Applied Energy 186 (2017) 189–196
55. Rajeev Pratap Singha, Pooja Singh, Ademir S.F. Araujo, M. Hakimi Ibrahim, Othman Sulaiman. Management of urban solid waste: Vermicomposting a sustainable option. Resources, Conservation and Recycling 55 (2011) 719–729
56. Hui Zhou, YanQiu Long, AiHong Meng, QingHai Li, YanGuo Zhang. Interactions of three municipal solid waste components during co-pyrolysis. Journal of Analytical and Applied Pyrolysis 111 (2015) 265–271
57. Leo Jaymee de Vilas Boas da Silva, Ivan Felipe Silva dos Santos, Johnson Herlich Roslee Mensah, Andriani Tavares Tenorio Gonçalves, Regina Mambeli Barros. Incineration of municipal solid waste in Brazil: An analysis of the economically viable energy potential. Renewable Energy 149 (2020) 1386e1394
58. ABNT – ASSOCIAÇÃO BRASILEIRA DE NORMAS TÉCNICAS. NBR 10004: Resíduos Sólidos – Classificação. Rio de Janeiro, 2004.
59. Hossein Ghanavati, Iraj Nahvi, Keikhosro Karimi. Organic fraction of municipal solid waste as a suitable feedstock for the production of lipid by oleaginous yeast Cryptococcus aerius. Waste Management 38 (2015) 141-148
60. Zhen-shan Li, Fan Fang, Xiao-yu Tang, and Ning-sheng Cai. Effect of Temperature on the Carbonation Reaction of CaO with CO_2. *Energy Fuels* 2012, 26, 4, 2473–2482
61. Atul Kumar, S.R. Samadder. A review on technological options of waste to energy for effective management of municipal solid waste. Waste Management 69 (2017) 407–422
62. Renz M. Ketonization of Carboxylic Acids by Decarboxylation: Mechanism and Scope. European Journal of Organic Chemistry, 2005. 979-988 (6)